# INTERACTIONS BETWEEN MOLYBDENUM DISILICIDE AND SOME METALLIC SYSTEMS



by

CARLOS A. BOTTREL COUTINHO



ProQuest LLC.
789 East Eisenhower Parkway
P.O. Box 1346
Ann Arbor, MI 48106 – 1346

To my parents

T-1432

A Thesis submitted to the Faculty and the Board of Trustees of the Colorado School of Mines in partial fulfillment of the requirements for the degree of Master of Science in Metallurgical Engineering.

Signed: Carlos A. Bottrel-Coutinho

Carlos A. Bottrel-Coutinho

Golden, Colorado

Date: December 22, 1971

Approved: Walter L. Bradley

Walter L. Bradley
Thesis Advisor

John P. Hager

John P. Hager
Head of Department
Metallurgical Engineering

Golden, Colorado

Date: December 22, 1971

## ABSTRACT

This investigation was conducted to determine the interactions (1) between $MoSi_2$ and the high-temperature materials Ni and Ni-Cr and (2) between the same silicide and the lower-melting materials Cu, Sb, Zn, Cd, Sn, Al, and Al-alloys.

$MoSi_2$ bars were prepared by cold-pressing and sintering 1-micron $MoSi_2$ powders.

The interactions were initiated by attempting to infiltrate the silicide bars with the molten metals or alloys.

The high-temperature interaction products were analyzed by hardness measurements, metallographic examination, optical emission spectrography, x-ray spectrometry, and x-ray diffraction.

The interaction between $MoSi_2$ and liquid Ni-Cr resulted in the formation of two other silicides, MoNiSi and $Ni_{16}Cr_6Si_7$. The interaction between $MoSi_2$ and Ni (this latter either in the liquid or solid state) resulted in the formation of MoNiSi.

A thermodynamic calculation for the Mo-Ni-Si system confirmed the stability of the compound MoNiSi at lower temperatures.

An approximation for the free energy of formation of MoNiSi was derived:

$$\Delta G^{o}_{MoNiSi} = -38,980 + 16.46\ T$$

Metallographic examination of the ceramic-metal interfaces showed that very little or no interaction occurred between $MoSi_2$ and the lower-melting metals and alloys in all the systems studied.

TABLE OF CONTENTS

# LIST OF FIGURES

## ACKNOWLEDGMENTS

The author wishes to express his appreciation to

- Dr. Walter L. Bradley, for his guidance and constant encouragement;

- Mr. Laurence E. Ferreira, Director of the Glendale Research Center, Interpace Corporation, who patiently initiated the author in the difficult and fascinating field of ceramics;

- the Brazilian Government, for the financial support provided;

- his professors and fellow students at Colorado School of Mines for their helpful suggestions during the development of this investigation.

# INTRODUCTION

The need for materials capable of working at high temperatures has brought forth, since World War II, a great volume of research and subsequent development of a series of alloys, ceramics, and cermets. Examples of these are the cobalt and nickel-base superalloys, which have been developed primarily for turbojet applications requiring high creep-rupture strength and corrosion resistance at temperatures of the order of 1800°F (980°C), and titanium carbide cermets (TiC with varying additions of Ni, Co, Cr, Mo, W, and other metals), used for gas-turbine nozzle vanes and buckets, integral turbine wheels, etc. (Clauss, 1969).

Considerable research was also undertaken in the 1950's, with the purpose of studying the possibilities of refractory metals (mainly Mo, Nb, and W) and their alloys. However, for most potential high-temperature applications, poor oxidation resistance limited the use of these metals. Through alloying, some success was obtained in reducing the oxidation rates of these materials, but with the

result that the alloys had lower strength and poorer fabricability.

At present, there seems to be a trend toward the development of cermets for applications at temperatures well above 2000°F (1090°C), for which the materials now available do not have the necessary properties. It is highly desirable for a material to be able to work at higher temperatures, as, for example, in gas turbines, because the efficiency and power of these turbines increase significantly with the gas inlet temperature.

The potential value of a cermet is the possibility of combining the high-temperature oxidation resistance and strength of ceramics with the ductility and impact strength of a metal or alloy. It is apparent that a ceramic part to which a metal addition is made will have its "ceramic" properties—high-temperature strength and oxidation resistance—somewhat decreased. The problem, therefore, is to find an "optimum" combination (types and relative amounts of ceramic and metallic phases) for the envisaged application. Such an investigation has been done for some cermets, e.g. TiC cermets (Glaser, 1955). Silver (or silver alloy) infiltrated oxides constitute another example of cermets developed for high-temperature applications (Williams, 1965).

The purpose of this investigation was to study the

interactions of molybdenum disilicide with several metals and alloys, in order to determine the possibility of developing a $MoSi_2$-based cermet capable of working at elevated temperatures with a reasonable combination of high-temperature strength and room-temperature ductility.

# THE INFILTRATION TECHNIQUE

## Historical Development

Composite cermetallic structures can be fabricated by sintering ceramic powders into a porous compact and then filling the pores with molten metal. Certain metals and alloys have been observed to diffuse into a compact and to occupy all the continuous pore volume. The resulting structure is unusual, in that both ceramic and metal phase may be continuous.

According to Goetzel and Shaler (1964), infiltration work was initiated during and immediately after World War I, when Leiser and Gebauer, in 1914-17 successfully infiltrated copper into porous iron, and Baumhauer, in 1922, infiltrated a porous body of tungsten carbide with a metal of the iron group. These first attempts, however, yielded fairly porous products, which did not find immediate industrial application. Copper-infiltrated iron was first made dense in 1929 by P. Melchior.

Some 15 years later, by addition of carbon and the application of heat treatment, high-strength

copper-cemented steel parts were developed for load-carrying components in household appliances and power plants. In the early 1950's, copper-infiltrated iron compressor blades for jet engines were produced at a rate exceeding 1 million per month. By 1962, the quantity of copper-infiltrated iron products made annually in the United States could be measured in thousands of tons.

In still another area the infiltration process has made an important contribution. Just after the development of cemented carbides for cutting tools, the need arose for heavy-duty electrical contacts. The ideal solution for these electrical contacts would be to combine the hardness and resistance to wear of refractory metals, such as molybdenum and tungsten, with the good thermal and electrical conductivities of the conductor metals silver and copper. This was accomplished simply by infiltration of silver or copper into the former metals, with great simplification of fabrication conditions. Solubility of the refractory metals into the liquid conductor metals is insignificant, but their interface energies are low enough for wetting to occur.

Baumhauer's approach—using infiltration as the means of introducing a binder into cemented carbides—remained semiforgotten for twenty-five years. It was

tried again when the advent of jet propulsion required new materials for turbine blades. Limits in creep resistance of nickel- and cobalt-based superalloys invited attention to the stronger and more creep-resistant cemented carbides and other refractory compounds. These, however, had two major disadvantages: poor oxidation resistance and inadequate ductility and thermal shock resistance. The first difficulty was overcome by replacing the pure binder by metals with more oxidation-resistant alloys, and by substituting titanium carbide for the more conventional tungsten carbide, thus giving birth to TiC-base materials with Ni-Co-Cr alloy binders. The second disadvantage was more difficult to solve, and it was in this area that infiltration made an important contribution. Through infiltration, both the ceramic and metallic phases could be made to be continuous, and in some practical instances this significantly improved the ductility of the material, as will be mentioned in the discussion of results obtained by previous investigators.

## Wettability

A usual approach to the practical and theoretical aspects of bonding in cermets is to consider the wettability of the solid phase by the liquid metal

component and the surface energies of the system. In this connection, assume that a liquid drop is placed in contact with a solid substrate, as shown in figure 1.

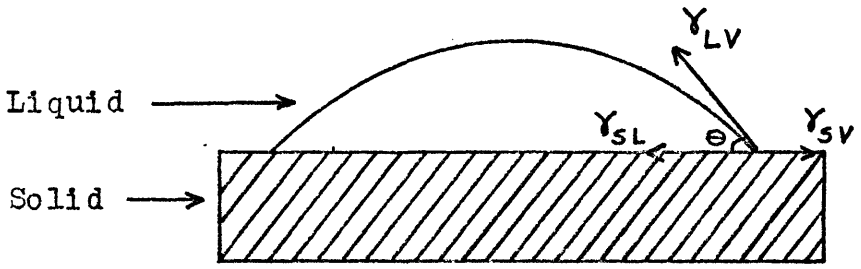


Figure 1. Surface forces acting at the intersection of a liquid resting on a solid with a contact angle $\theta$.

At the point of contact, A, of the liquid, solid, and gas phases, the contact angle, $\theta$, measured through the liquid phase is determined by the magnitude of the surface forces present, through the equation

$$\gamma_{SV} - \gamma_{SL} = \gamma_{LV} \cos \theta$$

where $\gamma_{SV}$, $\gamma_{SL}$, and $\gamma_{LV}$ are the surface energies, or tensions of the solid-vapor, solid-liquid, and liquid-vapor interfaces, respectively. Wettability, defined by

the contact angle, $\theta$, is a parameter that can be measured precisely. This simple parameter cannot be expected completely to describe the interactions taking place during fabrication of a cermet, but it can serve as a guide to the type of behavior to be expected, especially in liquid-phase sintering and infiltration.

The following effects of changes in the surface and interfacial energies on the value of the contact angle can be predicted from a consideration of the above relationship:

Complete wetting ($\theta = 0$), for example, cannot occur if $\gamma_{LV} > \gamma_{SV}$. Incomplete wetting—which results when $\gamma_{LV} > \gamma_{SV}$—is the situation in most pure metal/oxide ceramic combinations.

Another important aspect is related to surface contamination of the solid phase. If $\gamma_{LV}$ and $\gamma_{SL}$ remain constant, $\theta$ decreases as $\gamma_{SV}$ increases, and vice-versa. There is little possibility of markedly increasing $\gamma_{SV}$; hence, improvement in the wetting of solid oxides by molten metals is not likely to be obtained this way. However, the reverse is quite possible. This detrimental effect has been observed, for example, in a study of the wetting of titanium carbide by copper-nickel alloys, where slight oxygen contamination can considerably increase $\theta$. Fortunately, however, often the interactions

are more complex, and variations in $\gamma_{LV}$ and $\gamma_{SL}$ may also occur and result in increased wetting.

In both the initial choice of materials and the selection of a suitable method of fabrication, however, one should consider the wettability parameter with caution. The behavior of single components studied under ideal conditions may be far different from that of more complex real metal-ceramic systems, and even traces of contaminants may alter the entire wetting characteristics in a particular system. An aspect that should not be overlooked, for example, is that which Goetzel and Shaler (1964) call the "synergistic property" of contaminants or of detergents (chemical species added to the atmosphere or to the solid phase, with the purpose of modifying surface energies). This property consists in the experimental fact that the combined influences of two elements or substances can be much stronger than just the sum of the influences of the elements separately. This happens, for example, in infiltrating alumina with silver. Individually, an oxygen-containing atmosphere and the addition of copper have a slight detergent action; together they have a very strong action on the infiltration of silver into alumina, by significantly modifying the surface energies at play.

## Mechanism of Infiltration

The mechanism of infiltration is governed by the possible interactions between the high-melting solid phase (skeleton or "matrix") and the liquid metallic phase (infiltrant).

According to Goetzel (1960, p. 73-81), four different conditions can be distinguished:

1. the liquid does not wet the solid surface, and there is no solubility between the components;

2. wetting occurs but no solubility;

3. wetting occurs, and there is limited solution of the solid in the liquid component;

4. wetting occurs and there is complete solubility of either component in the other.

In the first case, contact angles and interfacial tensions are extremely high, and capillary action is inoperative. Only the use of external force makes it possible to drive the molten infiltrant through the interconnected pore structure of the matrix. Only in a few selected systems can the condition be overcome, at least in part, by the deposition of interfacial surface layers which tend to lower the contact angle. A good example is an oxide ceramic, such at $Al_2O_3$, plus a metal of the iron group or chromium. Materials that lower the

contact angle include copper oxide for nickel, and chromium oxide for chromium.

The second case is demonstrated by the duplex contact metal structure. Solution of the refractory metal in the molten conductor is practically nil, but the contact angles, between W and Cu, and between Mo and Si, for example, are very low. Hence capillary forces are the forces causing the occurrence of infiltration.

In the third case, diffusion processes plus liquid or plastic flow processes are in action besides the capillary forces. As the liquid passes through the capillaries, it tends to penetrate the regions where the solid particles form contact areas or grain boundaries. This penetration results in a preferred solution of these regions in the liquid. Isolation of the solid particles, amounting to a breakdown of the matrix, frequently occurs at the same time as a distinct spheroidization of the solid phase. Saturation of the liquid with the solute prior to infiltration inhibits spheroidization of the solid particles and avoids excessive material transport or cavitation. The precipitation-treatable alloys of iron and iron-carbon with copper and brass are typical materials of this category.

The fourth case is an expansion of the third. Diffusion processes occur to their maximum intensity

because of the unlimited solubility of the liquid and solid phases in each other. Temperature and time become predominant factors in the control of the process. Very short times of liquid phase action on the solid may permit retention of the geometry of the solid matrix, but prolonged times may result in liquefaction of the whole mass, with complete loss of the original configuration. This critical time, for a given temperature, is determined by the diffusion coefficient of the solute into the solvent. A simple example of this process is the nickel-copper system. Porous nickel can be infiltrated with molten copper in a few seconds, but dissolution of the matrix occurs almost instantaneously, so that solid bodies retaining their original shapes can be produced only by freezing the liquid progressively as soon as the liquid front has passed.

The systems based on chromium carbide ($Cr_3C_2$) plus nickel or cobalt are almost as difficult to control, and the saturation of the infiltrant metal with chromium or carbon does not significantly affect the process of solution.

## Infiltration Theory

The basic theory of interfacial phenomena in solid-liquid-gas systems is presented in Davies and

Rideal (1963). Using this theory and the infiltration model proposed by Kimura and others (1959), Williams (1965, p. 147-165) calculated the change in surface energy on infiltration, considering the porous ceramic matrix as a stable structure. The cermet will be stable with respect to the separate phases if the total surface energy is decreased during infiltration. In other words, infiltration will occur if

$$(A_L - A_e)\,\gamma_{LG} + A_i(\gamma_{SG} - \gamma_{SL}) > 0 \qquad (2)$$

where $A_L$ is surface area of the liquid before infiltration,

$A_i$ is area of the internal surfaces of the pores in the ceramic matrix,

$A_e$ is area of the external openings of the pores in the ceramic matrix,

and $\gamma_{LG}$,

$\gamma_{SG}$,

and

$\gamma_{SL}$ are specific surface free energies of the liquid-gas, solid-gas and the solid-liquid interfaces, respectively.

As $A_L$ and $A_e$ are small by comparison with $A_i$, equation 2 can be written as

$$A_i (\gamma_{SG} - \gamma_{SL}) > 0 \qquad (3)$$

The rate of infiltration is given by the Washburn-Rideal equation (Davies and Rideal, p. 419):

$$\frac{dl}{dt} = \frac{r(\gamma_{SG} - \gamma_{SL}) \cos \theta}{4 n e} \qquad (4)$$

where r is the mean radius of the pores,

l is the distance penetrated,

n is the viscosity of the liquid at the infiltration temperature, and

$\theta$ is the contact angle.

The rate of infiltration is proportional to the pore size. A decrease in pore size decreases the rate of infiltration, but, on the other hand, favors the process thermodynamically, because $A_i$ increases as r decreases.

Shaler (1965, p. 3-14) has suggested a very interesting quantitative theory based on a simplified infiltration model.

According to him, five conditions are necessary and sufficient to insure penetration of a liquid into a porous body:

1. a force, subsequently applied to the liquid on one side of the body would be required to expel the liquid, once infiltration has occurred;

2. the post-infiltration system has a lower free-energy (or surface free energy, all other factors being equal) than the pre-infiltration system;

3. the time required to accomplish essentially total penetration of the porous body, to be economical, must not be too long;

4. the liquid and solid must not react to form a solid compound or alloy having a specific volume as great as or greater than their combined pre-infiltration specific volume; otherwise, the reaction product blocks the entry of additional liquid before infiltration is complete; and

5. during solidification, the volume changes and the expulsion of gases from the liquid must not result in the formation of excessive porosity nor in the expulsion of too much of the infiltrated liquid.

The first two are thermodynamic conditions and the last three refer to practical aspects of the problem.

For the development of his theory, Shaler used the concept of an "index of infiltration," defined by Kimura and others (1959), which is representative of the tendency for infiltration to occur spontaneously. This index is equal to the difference between the sums of all the surface free energies of the system before and after infiltration. The index is a function not only of the

specific free energies of the various surfaces and interfaces considered, but also of the geometries of these surfaces. In a simple system, conditions 1 and 2 mentioned above essentially imply that the infiltration index must be positive, and the capillary pressure will then be a simple function of a derivative of the index.

The behavior of liquids being infiltrated into porous bodies having complex geometries, as most real bodies have, is not so simple, however. There are, for example, points of metastable equilibrium past which a positive external perturbation is necessary to move the system, even if in the end the completely infiltrated body has a lower total free energy. Put in other words, one or several steps of the infiltration process may require an "activation energy" for infiltration to go to completion. Some of these points of metastable equilibrium require fulfilling conditions 3, 4, and 5 mentioned above.

Shaler defined an "idealized" system, which is the basis for his infiltration theory. This system is one in which the porous body consists of a semi-infinite plate of otherwise dense and homogeneous solid material except for the presence within it of a regularly distributed bundle of straight smooth-surfaced cylindrical pores.

All the pores have the same radius and all are perpendicular to the large faces of the plate. The liquid is supposed initially to be in the form of a layer of uniform thickness adjacent to the plate, and is dense and homogeneous. The quantity of liquid of the idealized system is exactly sufficient to fill all the pores. The solid does not contribute anything to the gas phase, and, like the liquid, has nothing absorbed upon it, not even the vapor of the liquid. The liquid has zero specific gravity, so that no hydrostatic pressure is involved. The liquid and solid have thermal expansion coefficients of zero.

Figure 2 indicates the various stages through which the system can pass before infiltration has been completed.

The quantities needed to define the geometry of the system fully are r, t, and $\emptyset$, respectively, the radius of the pores, the thickness of the plate, and the porosity of the solid (ratio of pore area to total solid area).

Besides these geometrical parameters, the calculation of the energy balance requires values of specific surface free energies, of a factor which defines the shape of the meniscus that is to be formed, and of the external pressures exerted on the liquid. $\gamma_{LV}$, the specific surface free energy of the surface of the liquid

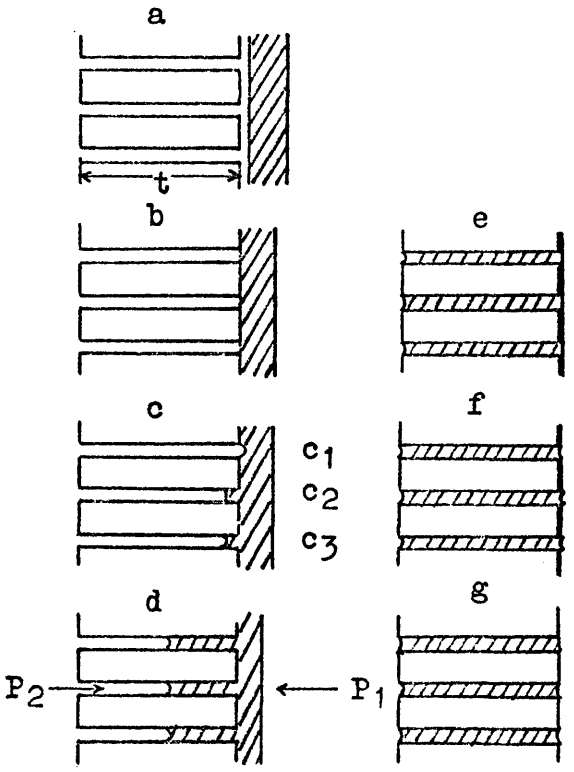


Figure 2. The possible stages of infiltration of a porous plate of very simple geometry (not all the configurations shown are necessarily real).

a. Initial state: liquid approaches solid.

b. Liquid in contact with solid.

c. Formation of first meniscus at each pore. The meniscus may be concave or convex outward as in $c_1$ and $c_2$ and its edge may be the edge of the pore, or not, as in $c_3$.

d. Partial penetration, expressed as fraction f of total penetration.

e. Liquid layer reduced to very small thickness.

f. Formation of second meniscus at each pore.

g. Disappearance of surface film.

in contact with its own vapor, and $\gamma_{SV}$, the specific surface free energy of the surface between the solid and the vapor of the liquid, are measurable properties. $\gamma_{SL}$, the specific surface free energy of the solid-liquid interface, can be determined by using Young's equation, if the contact angle $\theta$ is known:

$$\gamma_{SL} = \gamma_{SV} - \gamma_{LV} \cos \theta$$

The surface of the meniscus formed by the liquid in a pore is assumed to be spherical and to have the area $2\pi r^2(1 + \sin \theta)$.

Two external pressures, $p_1$ and $p_2$, are assumed to be acting on the liquid, one favoring infiltration and the other resisting infiltration (figure 2d.). The areas over which $p_1$ and $p_2$ act are, respectively, $\pi r^2/\phi$ and $\pi r^2$. When the liquid moves a unit distance in the pore, the thickness of the liquid layer changes by $\phi$ units; therefore, the work done is

$$\frac{\pi r^2}{\phi} (p_1 - p_2) \cdot \phi = \pi r^2 (p_1 - p_2)$$

The tendency for the system to go from one given stage of infiltration to the next—for example, from stage a to stage b (figure 2)—will be indicated by the index of infiltration $I_{ab}$, which corresponds to this step.

The overall index of infiltration will be the value of I for the change from state a to any of the states e, f, or g. The calculations will reveal, in each case, the state at which infiltration will stop.

The value of each one of the indices of infiltration is the sum of all the surface energies in each stage. Each surface energy is equal to the product of a specific surface energy by the area of the surface considered. The difference between the sum of all the surface energies in, for example, stage a and stage b will be the index which corresponds to step a-b of the process. If this difference is positive, the change from the first to the second stage will be spontaneous. If it is negative, then its magnitude is the work that must be done by external forces to take the system from the first to the second stage.

After calculating the indices of infiltration for each step ($I_{ab}$, $I_{bc}$, $I_{cd}$, $I_{de}$, $I_{ef}$, $I_{fg}$) and adding all these "component" indices, Shaler arrived at the following expressions for the overall index of infiltration:

$$I_{ae} = 2\pi r^2 \left\{ \left[ \frac{1}{2}\left(\frac{1}{\phi} - 1\right)(1+\cos\theta) + \frac{1}{2} - \frac{1}{1+\sin\theta} + \frac{t}{r}\cos\theta \right] \gamma_{LV} + \frac{t}{2}(p_1 - p_2) \right\}$$

and

$$I_{ag} = 2\pi r^2 \left\{ \left[ \frac{1}{\phi} - \frac{2}{1+\sin\theta} + \frac{t}{r}\cos\theta \right] \gamma_{LV} + \frac{t}{2}(p_1 - p_2) \right\}$$

The value of I to be considered is $I_{ag}$, when it is positive. If $I_{ag}$ is negative, this means that step f-g is not favored and, since Shaler has shown that step e-f is always negative, the process will stop at step e and therefore $I_{ae}$ is the index to be considered.

Letting

$$p_1 - p_2 = 0$$

$$\frac{t}{r} = 10,$$

Shaler calculated I for several values of $\theta$, which are reproduced in figure 3. This figure shows that infiltration will be spontaneous for small values of the contact angle $\theta$, and that for high values of $\theta$ an external pressure is required for infiltration to occur.

The above treatment of the infiltration process, as the author of the theory well acknowledges, is extremely simplified, and cannot be expected to give accurate results in the study of porous real bodies, because it seems impossible to describe mathematically the geometry of these bodies, with their irregular distribution of pore size, tortuosities, interconnections, capillary dams, varying roughness of pore surface, etc.

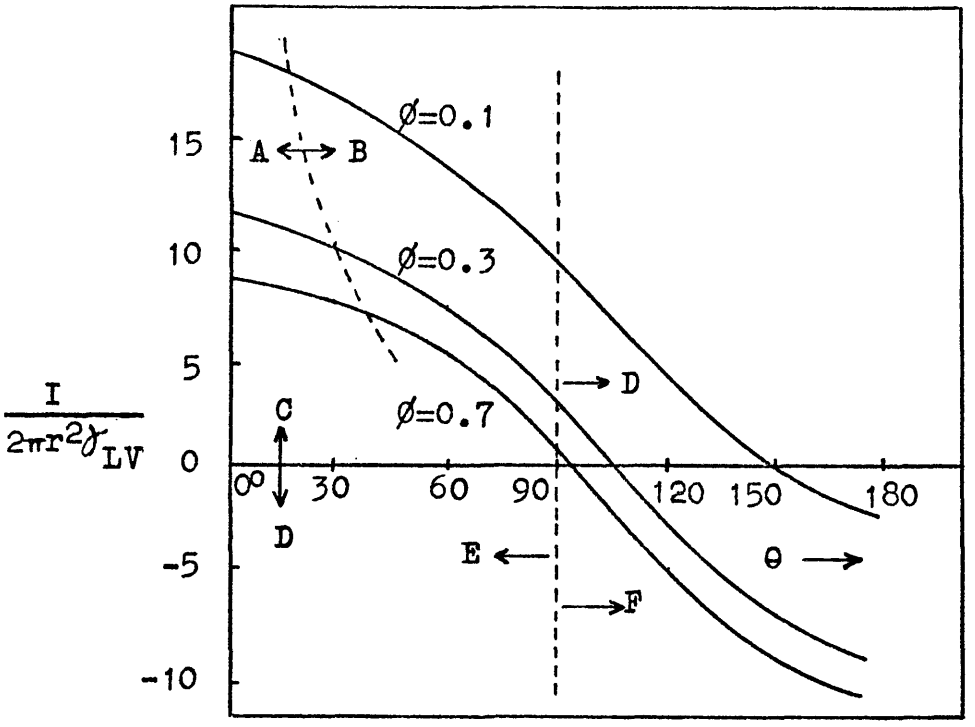


Figure 3. Overall index of infiltration vs contact angle.

$\frac{I_{ae}}{2\pi r^2\gamma_{LV}}$ or $\frac{I_{ag}}{2\pi r^2\gamma_{LV}}$ vs $\theta$ for $t/r = 10$ and

$p_1 - p_2 = 0$

A. Film remains;

B. Film disappears;

C. Spontaneous infiltration;

D. Infiltration requires pressure;

E. Infiltrant once in, stays in;

F. Infiltrant must be kept in by pressure during solidification.

Nevertheless, it can be a valuable model for qualitative predictions of the infiltration behavior of real systems.

## Infiltration Technique

Metal infiltration may be obtained essentially in three ways:

1. full submersion of the skeleton in the liquid metal bath;

2. capillary dip, whereby the skeleton is suspended while partially submerged in the bath;

3. contact (or superposition), where the skeleton is contiguous to a solid infiltrant body which liquefies during the process.

The first two methods were the ones used in early infiltration work. However, as there is a large amount of metallic residue in these procedures, economy has favored the selection of the third method in industrial production, as of iron-copper products.

With increasing ductility requirements, liquid phase proportions had to be raised to a point where it became necessary to devise mechanical support of the skeleton throughout the infiltration operation, for the retention of the original shape of the part.

industry. This system was developed in the 1940's by Goetzel and his co-workers, who used a copper-5% iron-5% manganese alloy as the infiltrant and steel as the skeleton body.

In the same decade, Krol and Goetzel (1949) developed high-temperature materials by infiltrating titanium carbide with a series of superalloys.

Within the scope of an investigation of cemented carbides produced by the infiltration process, Kieffer and Köebl (1950) systematically studied the infiltration of tungsten carbide, titanium carbide, molybdenum carbide (and also mixtures of these) by unalloyed metals, nickel-chromium, and cobalt-chromium and by these alloys presaturated with the carbides of the skeleton. From their experiments they arrived at the following conclusions:

1. If unalloyed metals, such as cobalt, iron, or nickel, are used as infiltrants, the formation of low-melting alloys with the carbide of the skeleton leads to deep pinholes at the surface from which infiltration takes place (method used was infiltration by superposition of the metal onto the carbide).

2. Presaturation of the infiltrant with the carbides of the skeleton almost completely prevents pinhole formation.

3. The pinhole formation in unalloyed infiltrant

## Advantages of the Infiltration Process

As pointed out by Goetzel and Shaler, the infiltration process has several favorable aspects:

1. attainment of virtually full density without need for excessive external pressure or work;

2. combination of two or more components of widely different melting points offering difficulties in casting or in sintering;

3. potential production of precise shapes even of large sizes by using proper molding, melting, heating and cooling techniques;

4. improvement of such surface characteristics as corrosion resistance and brazing and welding characteristics due to the presence of an infiltrant surface film integrally joined to the interior network;

5. improvement in machinability due to more favorable chip-breaking property of the skeleton material;

6. potential design of a wide variety of materials which can remain relatively cool in high-temperature service by auto-transpiration cooling.

## Results of Previous Investigators

Copper alloy-infiltrated steel was the first system to find commercial application in the metallurgical

metal increases with increasing solubility of the carbide in the respective metal.

4. After a short time of infiltration by superposition, the top layers of the material are denser and richer in binder metal than the bottom layers. A uniform distribution of the binder metal in the infiltrated material can be achieved by annealing at sintering temperature for several hours.

5. With increasing binder metal contents, the distribution of the binder metal becomes more uniform.

6. Carbides of comparatively low specific gravity permit the infiltration of 20 to 45 wt % of binder metal.

An important contribution in the field of infiltrated carbides was made by Goetzel and Adamec (1956, p. 101-106), when they introduced the so-called "graded" titanium carbide cermets. The term "graded" means that the metal composition in the cermet part varies along one or more directions so that the physical properties of any given section can accommodate the imposed mechanical and thermal conditions. This gradation provides ductility and toughness in areas which require these properties. In order to achieve this gradual change in metal content, the titanium carbide skeletons

were made with a varying green density, and after sintering, were filled with concentrations ranging from below 50 to above 80% by volume. Turbine buckets were produced in this manner, with a noticeably improved impact resistance. In their experiments, these investigators used various nickel alloys as binder metal.

Still in the field of cemented carbides, Goetzel and Skolnick (1956) developed a titanium carbide-base cutting material by infiltrating a titanium carbide skeleton with tool steel.

In the area of oxide-based cermets, the first materials produced by infiltration resulted from the experiments of Blakeley and White (1956). They started with preformed porous alumina bars coated with copper oxide, which were then infiltrated with silver and lower-melting silver-copper alloys, with very good results.

Graham and others (1963, p. 280-296) did extensive investigation on oxide-base cermets obtained by infiltration. Alumina and zirconia were the oxides used, and the infiltrants were silver or silver alloys (Ag-Pd and Ag-Pd-Cu). They arrived at some significant results, which can be summarized as follows:

1. The original cermet concept of primary dependence on a continuous ceramic network seems to be no

longer justified. Rather, a cermet may be considered a ceramic-modified metal, and although dispersion-strengthening theory has been developed mainly for low concentrations of the dispersed hard phase, it seems reasonable to extrapolate these strengthening mechanisms for more concentrated dispersions in the cermet range.

2. As a consequence of the aforesaid, matching of thermal expansions becomes a factor of secondary importance, provided the metallic phase is sufficiently ductile.

3. The degree of similarity between the infiltrated cermets and the concentrated dispersion-strengthened composites is not well defined. Although it appears that the ceramic network may remain more or less intact after infiltration, the network is certainly not intact after exceeding a critical strain, but the strength properties of the cermets are still impressive.

4. The observation of useful strengths up to the melting point of the metallic phase is particularly significant.

5. The change from mixed powder fabrication to infiltration allows greater control over structure and offers greater flexibility and economy from the perspective of production in quantity and in complex shapes.

Williams (1965, p. 147-165), one of the co-authors of the previous investigation mentioned, continued the research on oxides, extending it to magnesia and thoria, and also using another silver alloy (Ag-Pd-Pt). From his investigation, he was not able to confirm the previous hypothesis of the inevitability of disruption of the ceramic network, as the strength of his alumina skeletons was virtually unchanged after infiltration with silver. One important conclusion of his work was that using silver-20 or 30% palladium as infiltrant, alumina-base cermets retain useful strengths up to 1100°C. Also it was determined that large amounts of wetting agent, copper oxide, are required to achieve satisfactory infiltration with silver-20% palladium.

One current area where infiltration is being used is that of rocket-engine components that are exposed to high-velocity gas streams at temperatures that may exceed the melting temperature of the most refractory metals. The idea was to infiltrate a refractory metal with another lower-melting material in order to absorb these large amounts of heat without collapse of the component. This metal, through its fusion and vaporization, would provide a considerable cooling effect to the component, an effect which has been called "transpiration." Tungsten is

generally selected as the matrix material for such components, because of its high melting point. A number of relatively volatile metals such as copper, tin, lead, zinc, magnesium, and silver have been considered for dispersion in the tungsten matrix. Of these, silver has been most extensively evaluated and used in rocket-engine parts. Infiltration is the process used for dispersion of the lower-melting metal. The properties of silver-infiltrated tungsten have been extensively studied by Matt and Warga (1964), Goetzel and Rittenhouse (1964), and Dotson and Kotfila (1969, p. 1209-1227).

Gatti and others (1967, p. 13-24) have used the infiltration technique to obtain Al-$B_4C$/B/W continuous-filament composites. The ceramic matrix was made by vapor-depositing boron carbide over a boron filament having a tungsten-substrate core. By infiltration with aluminum, continuous-filament composites containing 50% in filament volume were obtained.

As already mentioned, important information can be obtained from wettability studies for finding metal-ceramic systems where infiltration can be used successfully as a technique of cermet preparation. Much experimental work has been done in this area. Allen and Kingery (1959,

p. 30-37) studied the wetting behavior of tin and tin-titanium alloy on $Al_2O_3$, SiC, $Si_3N_4$, and $MoSi_2$, determining that the addition of titanium to tin always lowers the contact angle, and very markedly for $MoSi_2$.

Manning and Stoops (1968, p. 415-419) performed wetting tests with several refractory metal-ceramic combinations. Sessile-drop contact angles between liquid Cr, V, Pt, Rh, Mo, and Mo-Re alloy and solid $ThO_2$, $HfO_2$, $ZrO_2$, HfC, TaC, and ZrC were measured at temperatures up to 2800°C. Little wetting occurred between the metals and the refractory oxides, but Mo and Mo-Re alloy did wet the carbides HfC and ZrC.

Samsonov and others (1968, p. 42-48) measured the contact angles of several liquid metals with carbides of group iv-vi transition metals. From their results, they suggest that, at least for refractory carbides, wetting cannot be regarded as only a surface phenomenon, disregarding the effect of the bulk. Rather, the electronic structure of both the refractory compounds and the wetting metals has to be considered.

Wettability studies of SiC single crystals by molten Cu, Ag, Au, In, Ga, Ge, Sn, Si, and Ni have been made by Naidich and Nevodnik (1969, p. 2066-2070). It

was determined that metals having a moderate chemical affinity towards carbon or silicon wetted the SiC surface readily.

The wetting of periclase, quartz, and sapphire by In, Ga, Sn, and Ag has been studied by Harding (1968), who measured the contact angles, work of adhesion, and interfacial free-energies of these systems.

# EXPERIMENTATION

## Cold Pressing

### Equipment

The cold pressing of the silicide powder was performed in an Instron tension-compression tester, model TT, 20,000 pounds.

The die used (figure 4) was a hardened alloy steel die, chrome-plated. The fixed dimensions of the compact are 2 1/2 x 13/32 in. (64 x 10.5 mm). The usual thickness of the samples made was 3/8 in. (9.5 mm).

### Procedure

The first attempts to cold-press $MoSi_2$ powder were made by mixing it with 1.5 to 3 w/o of stearic acid as a binder.

After several experiments, a pressure of 12,000 psi (840 $kg/cm^2$) was found to give a good compact.

However, when the compacts were heated for sintering, the presence of the binder became inconvenient.

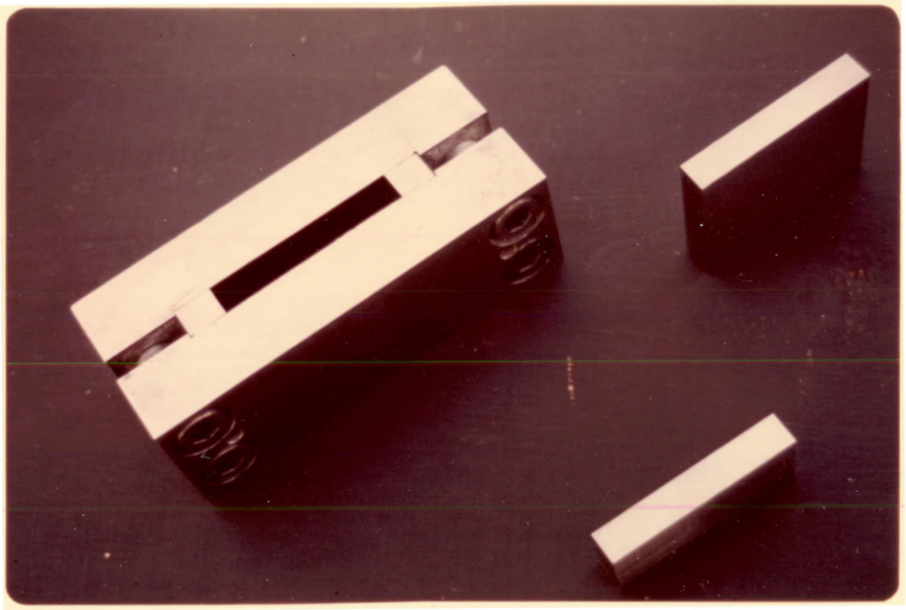

Figure 4. Alloy-steel chrome-plated die used for cold-pressing the $MoSi_2$ samples.

As it was burned, a deposit formed on the walls of the sintering Vycor chamber, which made it impossible to control the temperature by the optical pyrometer.

For this reason the binder was eliminated, and pure $MoSi_2$ powder was cold-pressed, at the same pressure of 12,000 psi. As a result, ejection of the sample from the die without spalling of the compact became difficult. This problem was solved by slightly lubricating the die walls with paraffin.

In some of the compacts, lamination occurred, always in the longitudinal direction of the sample. To correct this, the powder was stacked in the die very carefully, to obtain uniform distribution of the powder. Also, several speeds of loading were tried, but it was not possible to determine the influence of loading speed on the lamination, because the results were not consistent.

A typical green density, obtained at 12,000 psi (840 $kg/cm^2$), was 2.87 $g/cm^3$ (the theoretical density varies from 4.9 to 6.02 $g/cm^3$, depending on impurity content).

## Sintering

### Equipment

The sintering experiments were performed in a high-frequency induction-heating furnace (figure 5).

The generator used was a Westinghouse 10-KW radio-frequency generator, with a nominal frequency of 400,000 cps, a maximum voltage of 1,000 V and a maximum radio-frequency current of 450 amp.

Two different primary coils were used, both made of copper tubing 6.5 mm (1/4 in.) in diameter. Both coils were about 88 mm (3.5 in.) in diameter, one with an inductance of 0.219 $\mu$h and the other with an inductance of 0.351 $\mu$h.

The susceptor was a graphite crucible which heated the ceramic compact by radiation. The crucible sat on an evacuated Vycor container thermally shielded from the graphite crucible by two mullite tubings and a few alumina discs. Both the Vycor container and the primary coil were water-cooled.

### Selection of a Sintering Temperature

Amberg (1961, p. 102) reports a temperature range of 1250 to 1500°C for a $MoSi_2$-$Al_2O_3$ mixture in a hydrogen atmosphere, for 2 1/2 hr. of treatment.

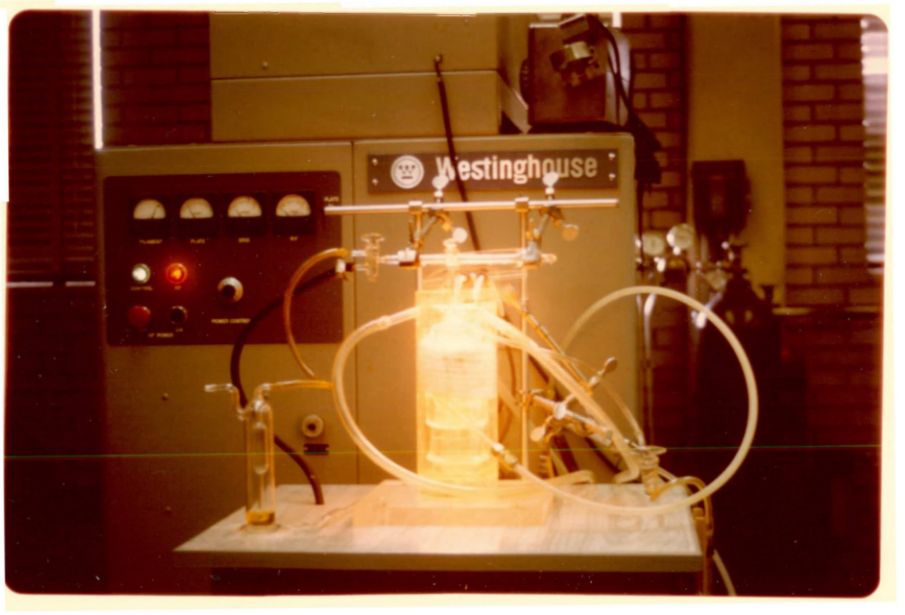


Figure 5. High-frequency induction-heating furnace.

However, since this datum does not refer to pure $MoSi_2$, a calculation was made to predict an approximate sintering temperature for $MoSi_2$.

A well-known sintering temperature of a ceramic material, that of $Cr_3C_2$, was taken as the basis for this calculation. According to Pozzo and West (1960, p. 151), the temperature range for sintering $Cr_3C_2$ is 1200 to 1350°C. The calculation was made assuming that the required vapor pressures for sintering $Cr_3C_2$ or $MoSi_2$ should be roughly the same.

Samsonov (1964, p. 111 and 121) gives the following equations for vapor pressures of Cr and Si in $Cr_3C_2$ and $MoSi_2$, respectively, as a function of the temperature T:

$$\log P_{Cr} = 6.525 - \frac{21,194}{T} \qquad (1)$$

$$\log P_{Si} = 28.62 - 5.75 \log T - \frac{29,800}{T} \qquad (2)$$

where P is pressure in atm

T is temperature in °K.

For T = 1200°C = 1473°K, equation 1 gives:

$$\log P_{Cr} = 6.525 - \frac{21,194}{1,473} = \bar{8}.13 ,$$

$$P_{Cr} = 1.35 \times 10^{-8} \text{ atm}$$

By iteration, a value for T in equation 2 that gives $P_{Si} \cong P_{Cr}$ can be found.

For the value T = 1400°C = 1673°K, equation 2 gives:

$$\log P_{Si} = 28.62 - 5.75 \times 3.224 - \frac{29,800}{1,673} = \bar{8}.27$$

$$P_{Si} = 1.86 \times 10^{-8} \text{ atm.}$$

For practical purposes $(P_{Si})_{T=1400°C} = (P_{Cr})_{T=1200°C}$.

Procedure

To check the validity of the calculated sintering temperature, one compact was sintered as follows:

a) heating from room temperature to 900°C in 1/2 hour,

b) heating from 900°C to 1400°C in 1/2 hour,

c) holding at 1400°C for 2 hours,

d) cooling to room temperature in 1/2 hour.

At the beginning of the experiment, the sintering chamber was purged several times with argon, to reduce the oxygen partial pressure inside the container. During the experiment, a flow of argon was maintained through the sintering chamber.

The result is shown in figure 6, left. The presence of considerable bloating indicates an excessively high sintering temperature and/or oxidation.

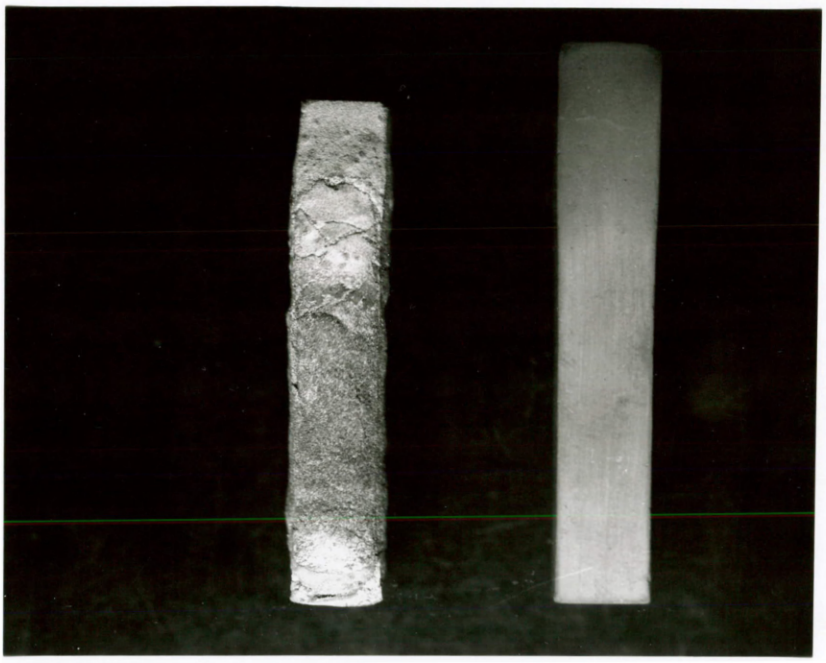

Figure 6. Sintered $MoSi_2$ samples. Left: sample sintered for 2 hr. at 1400°C, showing oxidation and bloating. Right: sample sintered for 2 hr. at 1100°C. 1.5 x.

To correct this, lower sintering temperatures were used. The temperature range 1050-1100°C was determined to produce well sintered samples. One of these is shown in figure 6, right.

It is possible that the successful sintering at a temperature considerably lower than predicted was promoted by the presence of C and N as impurities in the silicide (see appendix 2).

The average density of the sintered samples was 5.8 $g/cm^3$, in very good agreement with the value of 5.82 $g/cm^3$ given by Wehamann (1967, p. 423) for a material containing similar content of impurities, also cold-pressed and sintered.

Because of insufficient height of the primary coil of the induction furnace, the samples were subject to a temperature gradient. As a consequence, one end of the samples was incompletely sintered. This was corrected by designing a longer coil, as already mentioned.

A micrograph of a sintered sample is shown in figure 7.

## Infiltration

### Equipment

Two furnaces were used for the infiltration experiments:

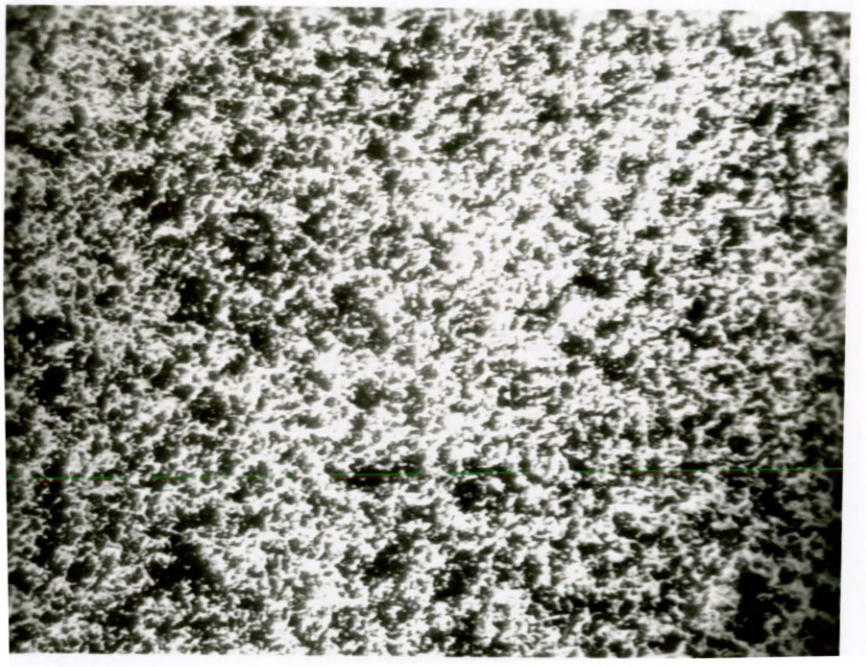

Figure 7. Sintered $MoSi_2$. Relatively high porosity, considered as a favorable condition for infiltration. Unetched. 280 x.

1. an induction furnace, the same used for sintering, and

2. a Haynes muffle furnace, heated by globar elements, maximum temperature of 1315°C (2400°F).

The induction furnace was used for the infiltration with nickel and nickel-chromium alloy, and the muffle furnace was used for the infiltration with lower-melting metals and alloys.

Procedure

Infiltration with Ni and Ni-Cr Alloy -- The sintered sample and the nickel or nickel-chromium alloy were weighed and heated in the induction furnace. The materials were contained in an alumina crucible.

The furnace was heated to 1480°C (2700°F) and 1510°C (2750°F), respectively, for the nickel-chromium and the nickel infiltration.

The system was held above melting temperature of the metal for 40 min., in both cases, under a positive argon pressure. The furnace was then cooled slowly, and the samples were again weighed. The mass balance is presented in table 1.

In both infiltration experiments the sintered silicide bar lost its original configuration, being, as it were, "dissolved" by the molten metal or alloy.

TABLE 1

Mass balance of the infiltrated systems.

| System | Weight, g | | Weight Loss, g |
|---|---|---|---|
| | Before Experiment | After Experiment | |
| Ni-Cr, $MoSi_2$ | 21.10 | 20.74 | 0.36 |
| Ni, $MoSi_2$ | 20.81 | 20.62 | 0.19 |

At this point it should be mentioned that the initial idea was to try to infiltrate with Ni-Cr only. It was because of the unexpected "dissolution" of the $MoSi_2$ in the Ni-Cr that infiltration with Ni was also tried.

Infiltration with Lower-melting Metals and Alloys -- Infiltration was also attempted with several lower-melting metals and alloys: pure Al, Al 2014, Al 4043, Al 5056, Al-6%Ti, Al-10%Ti, pure Cu, Sb, Zn, Sn, and Cd. The compositions of these metals and alloys are given in appendix 1.

The metal or alloy and the $MoSi_2$ were heated 100 to 450°C above the melting temperature of the metal or

alloy, and held at this temperature for about 5 min. According to Graham and Williams (1963), if infiltration occurs, it does not take more than a few seconds; therefore, a 5-min. exposure was considered long enough. The idea of superheating the metal or alloy is based on the results obtained by Allen and Kingery (1959, p. 35) when determining contact angles of liquid tin with $MoSi_2$: the contact angle was found to decrease significantly with increasing temperature of the liquid metal.

The experimental conditions are given in table 2.

## Analytical Work

### Hardness Measurements

Rockwell A hardness measurements were made of the sintered silicide and of the products of the interaction with nickel and nickel-chromium. The average values are shown in table 3.

TABLE 3

Rockwell A Hardness of Systems Studied.

| System | Rockwell A |
|---|---|
| $MoSi_2$, sintered | 76 |
| $MoSi_2$ + Ni | 74 |
| $MoSi_2$ + Ni-Cr | 74 |

TABLE 2

Experimental Conditions in the Infiltration with Lower-melting Metals.

| Metal or Alloy | Melting Temperature, °C | Temperature in Experiment, °C | Superheating °C | Time at Temperature, Minutes |
|---|---|---|---|---|
| Al 99.999% | 660 | 930 | 270 | 15 |
| Al 2014 | 510-638 | 920 | 280 | 10 |
| Al 4043 | 577-620 | 920 | 300 | 15 |
| Al 5056 | 568-638 | 920 | 280 | 15 |
| Al-6%Ti | 665-1130 | 1250 | 120 | 10 |
| Al-10%Ti | 665-1200 | 1290 | 90 | 10 |
| Cu OFHC | 1083 | 1180 | 100 | 20 |
| Sb | 630 | 870 | 240 | 10 |
| Zn | 420 | 870 | 450 | 10 |
| Cd | 321 | 700 | 380 | 10 |
| Sn | 232 | 550 | 220 | 10 |

In the experiments with Al 4043, antimony, and cadmium there was apparently no interaction between the $MoSi_2$ and the metal: the ceramic sample and the solid metal simply came apart, indicating complete absence of cohesion.

The hardness of sintered $MoSi_2$ is in good agreement with the value of Rockwell A 74 given by Samsonov (1964, p. 182).

The hardness of the samples obtained using lower-melting metals are not mentioned, since the interaction between the $MoSi_2$ and each metal, if any, occurred only at the ceramic-metal interface.

Metallography

Metallographic samples were prepared from all the experiments conducted, except from the systems $MoSi_2$ - Al 4043, $MoSi_2$-Sb, and $MoSi_2$-Cd, for which no interaction occurred.

The samples were ground to sand paper 4/0, then finished in grade 1 and 3 alumina.

The micrographs are shown in figures 9 to 15.

X-ray Diffraction and Spectrometry

X-ray diffraction patterns, using Debye-Scherrer method, were made of the systems $MoSi_2$-Ni-Cr and $MoSi_2$ - Ni.

For a reason which will be mentioned later, an x-ray pattern was also made of a sample prepared by sintering a mixture of $MoSi_2$ and Ni powders.

Cu K$\alpha$ ($\lambda$ = 1.5405) radiation was used, at 40 kv and 20 ma, with an exposure time of 1.5 or 2 hr.

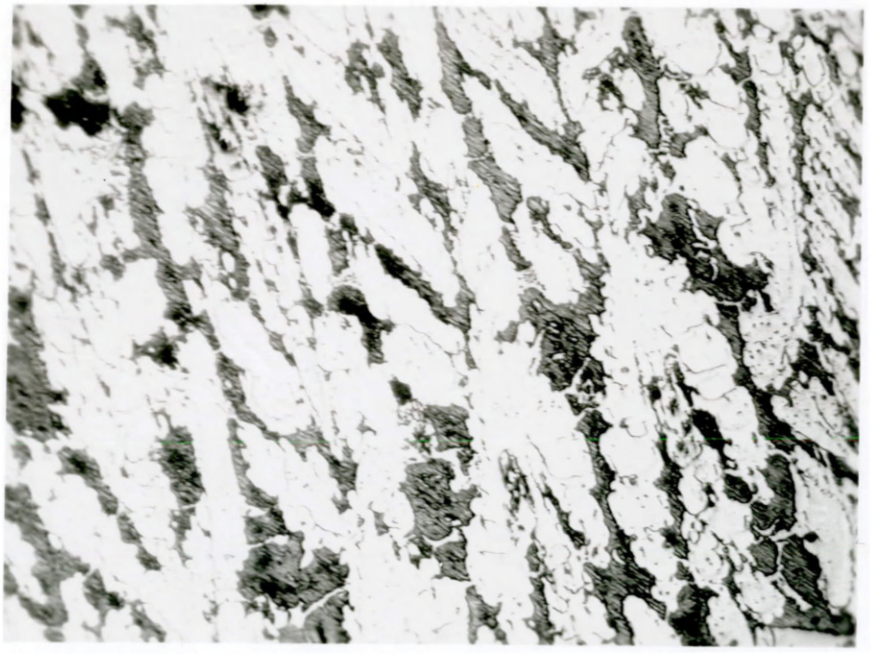

Figure 8. $MoSi_2$, Ni-Cr system. As-cast structure.
Etch: Keller's concentrated reagent. 90 x.

Figure 9. $MoSi_2$, Ni system. As-cast structure.
Etch: Keller's concentrated reagent. 110 x.

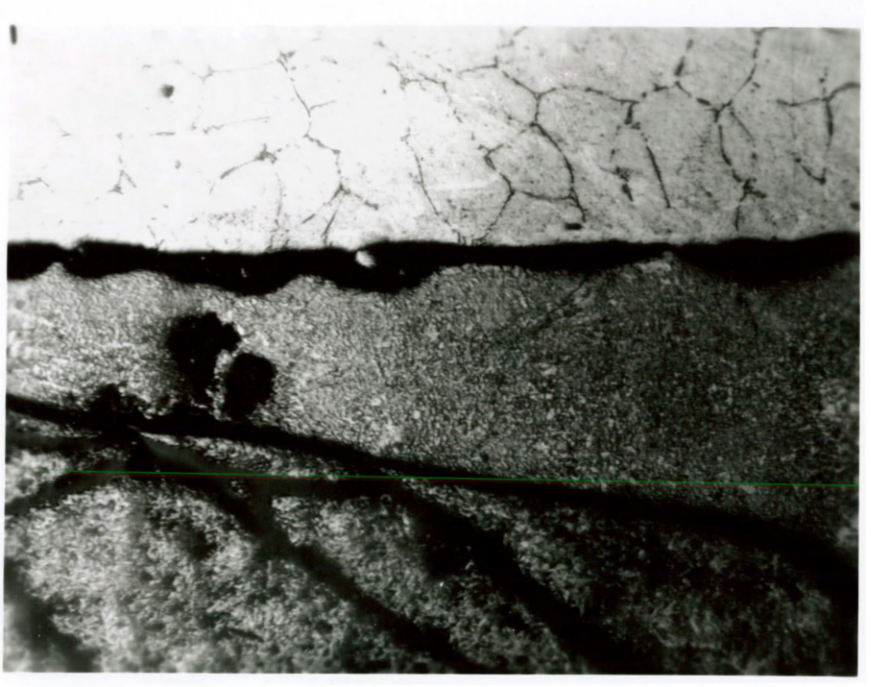

Figure 10. $MoSi_2$, Al system. Very little interaction occurred at the ceramic-metal interface.

Etch: Keller's reagent. 110 x.

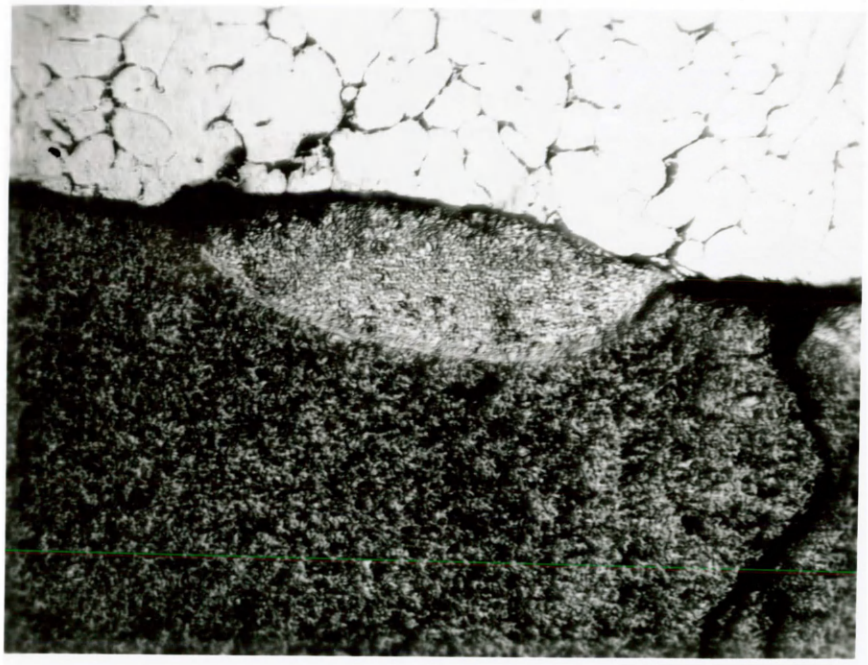

Figure 11. $MoSi_2$, Al-4.5% Cu system. Aluminum alloy shows cored dendrites of $\alpha_{Al}$ and probably some $\alpha_{Al} + \theta$ eutectic due to metastable equilibrium in relatively rapid cooling.

Limited interaction occurred at the ceramic-metal interface, in discrete ellipse-shaped regions, one of which is seen in photomicrograph.

Etch: Keller's reagent. 110 x.

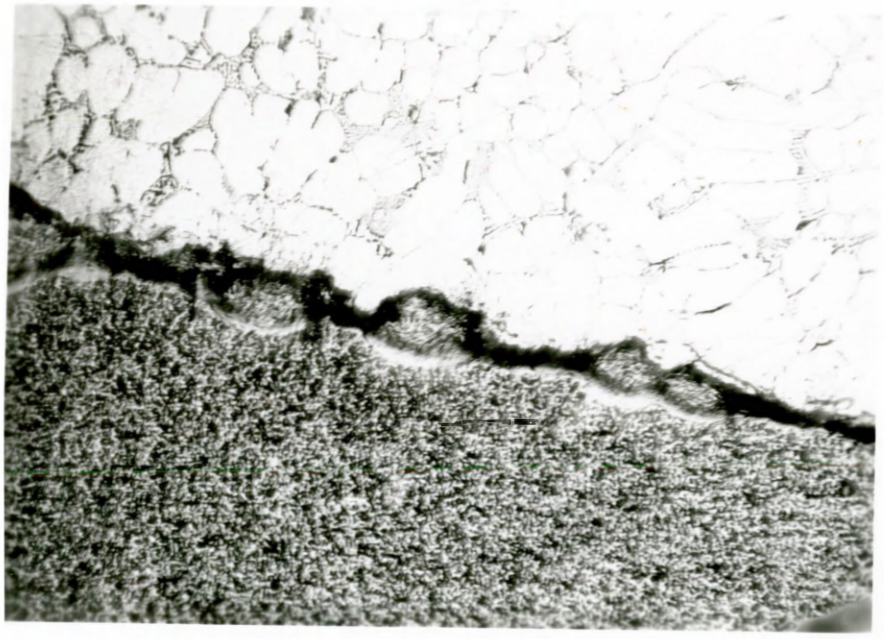

Figure 12. $MoSi_2$, Al-5%Mg system. Aluminum alloy has $\alpha_{Al}$ and eutectic structure due to metastable equilibrium in relatively rapid cooling.

Similarly to the Al-Cu, $MoSi_2$ system, limited interaction occurred at the ceramic-metal interface, in ellipse-shaped regions.

Etch: Keller's reagent. 110 x.

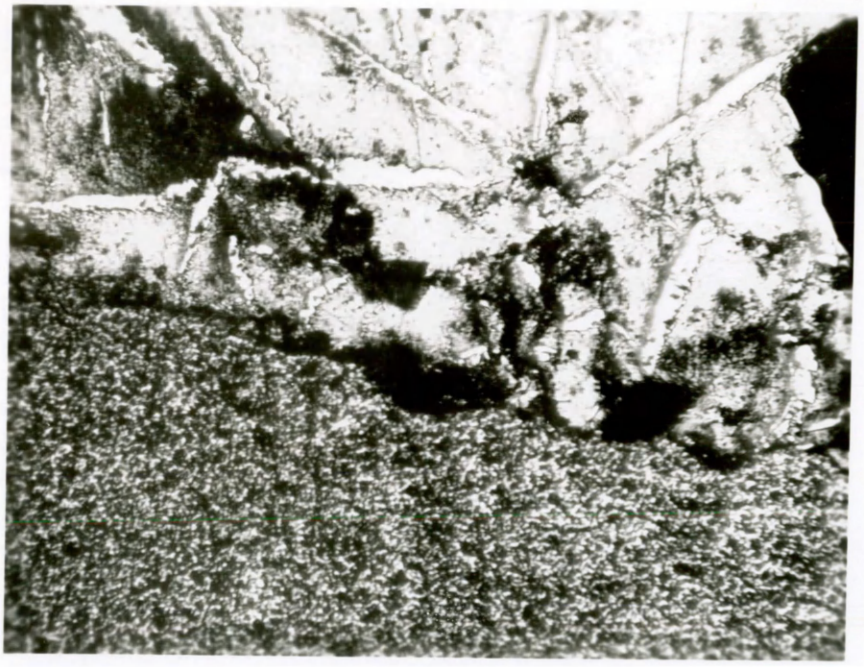

Figure 13. $MoSi_2$, Al-6%Ti system. Very little interaction occurred at the ceramic-metal interface.

Etch: Keller's reagent. 110 x.

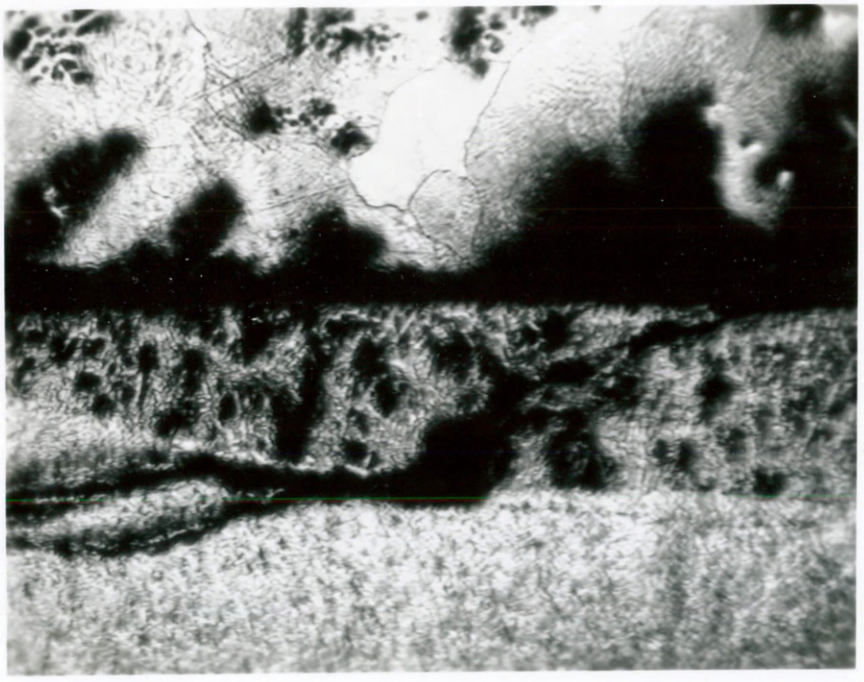

Figure 14. $MoSi_2$, Cu system. Limited interaction occurred at the ceramic-metal interface. The altered region at the interface is about 0.13mm thick.

Etch: ferric chloride. 180 x.

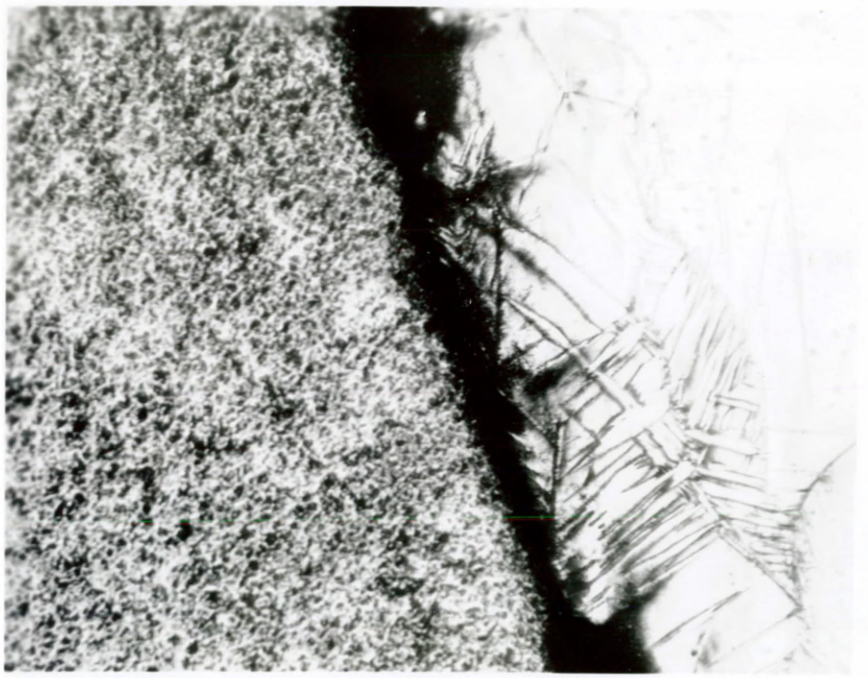

Figure 15. $MoSi_2$, Zn system. Very little interaction occurred at the ceramic-metal interface.

Etch: Palmerton reagent. 110 x.

The diffraction patterns, as well as the readings of the lines, are presented in appendix 2.

Qualitative x-ray spectrometry was also conducted on the $MoSi_2$-Ni-Cr system. Tungsten K$\alpha$ radiation at 45kv and 30 ma was used. LiF was the analyser crystal used. This analysis confirmed the presence of Mo, Cr, and Ni in the sample.

In both diffraction and spectrometry analyses, Norelco equipment was utilized.

Optical Emission Spectrography

In order to check the presence of Si, a spectrochemical analysis was made of the $MoSi_2$-Ni-Cr system, using a Baird grating spectrograph. The analysis indicated the presence of the major elements Mo, Si, Ni, and Cr, and of small amounts of Al and Mg. The presence of these impurities checks well with the composition of the Ni-Cr alloy given in appendix 1.

## ANALYSIS OF THE RESULTS

### $MoSi_2$, Ni-Cr System

Figure 7 shows that the sintered $MoSi_2$ is fairly porous, which was considered a favorable condition if infiltration in any of the systems studied was to occur.

When exposed to liquid Ni-Cr at about 1500°C, the ceramic sample was unable to retain its bar-like geometry, and the final shape of the system was that of its alumina crucible container. The quite unusual feature was that the temperature of the liquid alloy was about 500°C below the melting point of $MoSi_2$, which is 2030°C, according to Wehrmann (1967, p. 419).

The product had a metallic luster and showed no sign of oxidation. The mass balance presented in table 1 indicates a negligible weight loss.

The next steps in the analysis of the product were the hardness measurement and metallographic examination. The hardness was not significantly different from that of the silicide. The microscopic examination

did not bring much light to the problem, as figure 8 shows.

X-ray diffraction analysis was the next step. A powder pattern of the $MoSi_2$, Ni-Cr system was made. The result is shown in appendix 2.

The interpretation of the powder pattern showed that during "infiltration" experiment, two new silicides were formed: MoNiSi and $Ni_{16}Cr_6Si_7$. Also, the absence of lines corresponding to $MoSi_2$ and Ni-Cr in the pattern indicates that essentially all the starting materials were consumed to form the two new compounds. The "d" spacings given by ASTM for all the materials participating in the reaction are reproduced in appendix 2, for comparison with the values measured in the powder pattern.

The compound MoNiSi has been detected only recently. It was not referred to in previous studies of the Mo-Ni-Si ternary system, as, for example, those of Pfautsch (1925, p. 48-52) and Guard and Smith (1959, p. 283-287). Apparently, it was first detected by Gladyshevskii and Kuz'ma (1960, p. 66-71). These investigators were studying phase equilibria at 800°C and 1000°C in ternary alloys of the systems Mo-Fe-Si, Mo-Co-Si, Mo-Ni-Si, W-Fe-Si, W-Co-Si, and W-Ni-Si. These systems were investigated for the purpose of establishing

the presence of, and determining the properties of ternary compounds. The following phases were found: MoFeSi, MoCoSi, MoNiSi, WFeSi, WCoSi, and WNiSi. The technique of preparation of the alloys, for comparison with the present situation is worth mentioning. The mixtures were prepared by pressing together the pure metal powders and subjecting them to preliminary heating under argon. They were then heated in vacuum in closed quartz ampoules to 1100°C for 48 hr., then soaked at 800 to 1100°C for 150 hr. and quenched several times in cold water after repeated heatings. From x-ray diffraction studies, it was found that the ternary compounds are of the $MgZn_2$ type.

The above description shows that the MoNiSi was arrived at through a close-to-equilibrium reaction of the pure metals at a temperature relatively low ($\lesssim$ 1100°C). The present investigation shows that the same compound is obtained by a reaction between $MoSi_2$ and liquid Ni-Cr at a considerably higher temperature (1500° - 1550°C). One is, therefore, apparently in the presence of a new reaction.

The other silicide formed during this reaction was $Ni_{16}Cr_6Si_7$. The existence of this compound is reported by Gladyshevskii and Borusevich (1963), who also determined its structure and d spacings. These

latter values are reproduced in appendix 2.

The excellent agreement between the diffraction lines found for MoNiSi in the present investigation, and those reported by Gladyshevskii and Kuz'ma, leaves no room for doubt with respect to the formation of MoNiSi. The same cannot be said of the compound $Ni_{16}Cr_6Si_7$, also detected in the x-ray powder pattern. Here, three weak lines (of intensities equal to or less than 6%) reported by Gladyshevskii and Borusevich could not be detected in our pattern. However, considerable evidence of the presence of $Ni_{16}Cr_6Si_7$ led to the decision to make a mass balance of the system.

The initial total mass of 21.1 g of material was distributed as follows:

| | | |
|---|---|---|
| $MoSi_2$ | : | 9.1 g |
| Ni-Cr | : | 12.0 g |

or

| | | |
|---|---|---|
| Mo | : | 5.9 g |
| Si | : | 3.2 g |
| Ni | : | 9.4 g |
| Cr | : | 2.6 g |
| | | 21.1 g |

The weight loss during infiltration was considered, since it was very small, as already mentioned.

Assuming all Mo was consumed to form MoNiSi, a consumption of 1.74 g Si and 3.62 Ni would be needed. This would leave, then,

$$9.40 - 3.62 = 5.78 \text{ g of Ni,}$$

$$3.2 - 1.74 = 1.46 \text{ g of Si,}$$

and, of course, 2.6 g of Cr.

Assuming now that all Ni was consumed to form $Ni_{16}Cr_6 Si_7$, this would imply a consumption of 1.95 g Cr and 1.27 g Si. This consumption would then leave

$$1.46 - 1.27 = 0.19 \text{ g of Si}$$

$$2.6 - 1.95 = 0.65 \text{ g of Cr}$$

Summing up, the mass balance would be the following, assuming formation of MoNiSi and $Ni_{16}Cr_6Si_7$:

Initial materials:

| | |
|---|---|
| $MoSi_2$ | 9.1 g |
| Ni-Cr | 12.0 g |
| | 21.10 g |

Final materials:

| | | |
|---|---|---|
| $MoNiSi$ | 11.26 | g |
| $Ni_{16}Cr_6Si_7$ | 9.00 | g |
| Si | 0.19 | g |
| Cr | 0.65 | g |
| | 21.10 | g |

One can see that the hypothesis of the presence of $MoNiSi$ and $Ni_{16}Cr_6Si_7$ as the only final products is well supported by the mass balance. The very small amounts of Si and Cr appearing in the calculations (which represent, respectively, about 1% and 3% of the total weight) would be, quite likely, dissolved in one or in both silicides formed, giving slight deviation from stoichiometry.

The mass balance results in combination with the x-ray diffraction results support the hypothesis of a second silicide $Ni_{16}Cr_6Si_7$ beyond a reasonable doubt.

## $MoSi_2$, Ni System

In order to determine whether the presence of chromium has a major influence in the behavior previously described, infiltration of $MoSi_2$ with pure nickel was also tried. The experiment was performed at 1600°C, a

higher temperature than in the $MoSi_2$, Ni-Cr system, because of the higher melting point of nickel.

Here again the original silicide bar lost its original configuration and the final product, after the infiltration, was a metallic button.

Hardness measurement indicated a hardness of 74 Rockwell A, similar to that of $MoSi_2$ (76 Rockwell A).

An x-ray powder pattern was made, which is reproduced in appendix 2. The reaction products were identified as MoNiSi and Ni.

A mass balance, similar to that done for the $MoSi_2$, Ni-Cr system, showed that a significant amount of unreacted Ni was to be expected.

The formation of MoNiSi as a result of a reaction between $MoSi_2$ and liquid nickel suggested a thermodynamic calculation to determine whether this reaction could be confirmed thermodynamically. The simplifying assumptions made and the details of the calculations are given in appendix 4. It was possible to show that the compound MoNiSi is the stable compound, at lower temperatures ($<850^oC$), in the system Mo-Ni-Si. Its free energy of formation $\Delta G^o_{MoNiSi}$ is more negative than that of $MoSi_2$ at temperatures below $850^oC$. An original expression for $\Delta G^o_{MoNiSi}$ as a function of temperature was derived:

$$\Delta G^{o}_{MoNiSi} = 38,980 + 16.46\ T$$

The free energies of formation of $MoSi_2$ and Mo-Ni-Si are plotted in figure 16, where it can be seen that MoNiSi is the stable compound at lower temperatures.

## Mixture of $MoSi_2$ and Ni Powders

With the purpose of investigating whether the reaction of formation of MoNiSi from $MoSi_2$ plus Ni could occur also with both starting materials in the solid state, a mixture of $MoSi_2$ plus Ni powders (70% $MoSi_2$, 30% Ni) was cold-pressed and sintered for 2 hr. at 1050°C.

The sintered material was then examined by x-ray diffraction; the results are presented in appendix 2. The lines detected correspond to those of MoNiSi, $MoSi_2$, and Ni.

In this fashion it was possible to show that the reaction between $MoSi_2$ and Ni to form MoNiSi occurs also in the solid state, at temperatures as low as 1050°C. The fact that $MoSi_2$ and Ni are present after 2 hr. at 1050°C indicates that the rate of the reaction, as is to be expected, is considerably lower at lower temperatures (the time for reaction in the previous 3 experiments was less than 1 hr.).

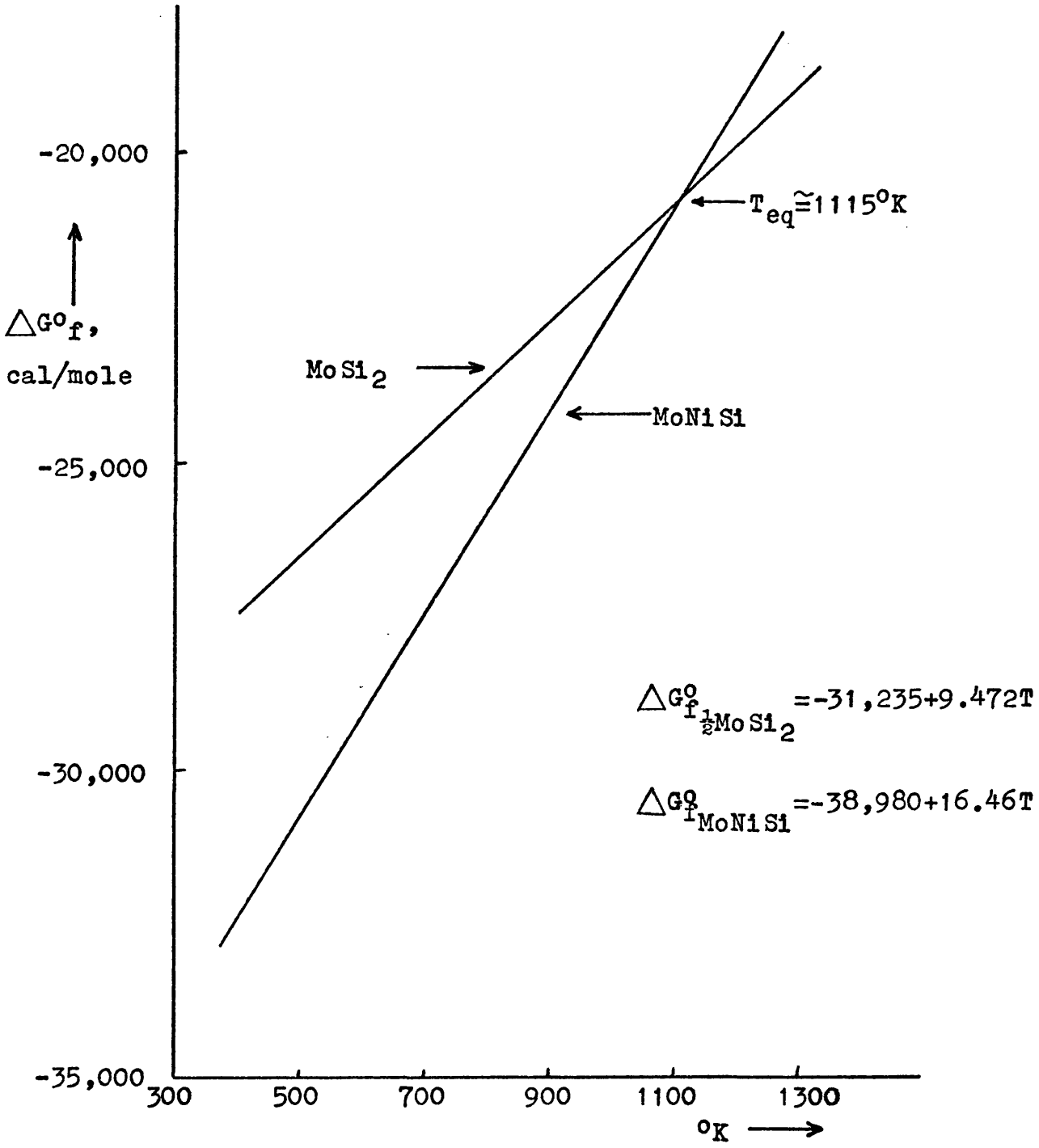


Figure 16. Free energies of formation of $MoSi_2$ and MoNiSi.

## $MoSi_2$ and Lower-Melting Metals

Interactions between $MoSi_2$ and several lower-melting metals and alloys were also studied by dipping sintered silicide samples in the molten metals. Infiltration was attempted with the pure metals that were available: Cu, Sb, Zn, Cd, Sn, and Al. Some Al alloys (Al-Cu, Al-Si, Al-Mg, and Al-Ti) were also studied, to determine the influence of alloying elements in the infiltration with aluminum.

Simple separation of the ceramic and the metal occurred for cadmium, antimony, and aluminum-silicon alloy.

Microphotographs of the systems $MoSi_2$-Cu, $MoSi_2$-Zn, $MoSi_2$-Sn, $MoSi_2$-Al-Cu, $MoSi_2$-Al-Mg, and $MoSi_2$-Al-Ti are shown in figures 10 to 15.

The photographs were taken at the interfaces ceramic-metal to determine whether any significant changes were observable in these regions. The examination of these interfaces showed that very little change occurred at the interface, and it was concluded that they were not significant enough to justify further analysis.

## CONCLUSIONS

The investigations made in this work made it possible to derive some conclusions with respect to the interactions between molybdenum dissilicide and several metals and alloys.

In the high-temperature systems $MoSi_2$-Ni-Cr and $MoSi_2$-Ni, the interaction ceramic-metal results in the formation of MoNiSi and $Ni_{16}Cr_6Si_7$ in the first system and of MoNiSi in the second. A thermodynamic calculation in the system Mo-Si-Ni showed that the silicide MoNiSi is the stable compound at lower temperatures, confirming the experimental data.

It was possible to derive an original expression for the free energy of formation of MoNiSi, given by:

$$\Delta G^{o}_{MoNiSi} = -38,980 + 16.46\ T$$

The formation of MoNiSi occurs with the reacting metal Ni in either the liquid or solid states, showing a considerably lower rate in the latter condition.

The interactions between $MoSi_2$ and the lower-melting metals and alloys Cu, Al, Sb, Zn, Cd, Sn, Al-Cu, Al-Si, Al-Mg, and Al-Ti were found to be either nonexistent or insignificant. When an interaction did occur (Cu, Al, Zn, Al-Cu, Al-Mg), it was limited to a very thin layer at the ceramic-metal interface. It should be emphasized that the validity of these conclusions is limited to the temperatures at which the infiltration tests were conducted.

## Appendix 1

### Chemical Composition of Materials Used

T-1432

| Material | Weight % | | | | | | | | | | | | | | | |
|---|---|---|---|---|---|---|---|---|---|---|---|---|---|---|---|---|
| | C | Mg | Al | Si | Ti | V | Cr | Mn | Ni | Cu | Zn | Mo | Cd | Sn | Sb | |
| $MoSi_2$ | | 0.4 | | 35 | | | | | | | | bal | | | | 0.23N, 1440 |
| 80-20NiCr | 0.031 | 0.062 | 0.063 | | | | 21.5 | | | | | | | | | |
| pure Al | | | 99.999 min | | | | | | | | | | | | | |
| Al 2014 | | 0.4 | bal | 0.8 | | | | 0.8 | | 4.4 | | | | | | |
| Al 4043 | | | bal | 5 | | | | | | | | | | | | |
| Al 5056 | | 5.2 | | | | | 0.1 | 0.1 | | | | | | | | |
| Al-6Ti | | | bal | 0.05 | 6.3 | 0.22 | | | 0.01 | | 0.02 | | | | | 0.1Fe |
| Al-10Ti | | | | 0.07 | | 0.41 | 0.01 | | 0.05 | 0.01 | 0.02 | | | | | 0.21Fe, 0.02Zn |
| Cu | | | | | | | | | | >99.5 | | | | | | |
| Sb | | | | | | | | | | | | | | | >99.5 | |
| Zn | | | | | | | | | | | >99.5 | | | | | |
| Cd | | | | | | | | | | | | | >99 | | | |
| Sn | | 0.5 | | | | | | | | | | | | bal | | 0.5Bi, 0.1Ca |
| Ni | | | | | | | | | 99 | | | | | | | |

## Appendix 2

### X-ray Diffraction Data of Materials Studied

| Infiltration | | | | Mixed Powders | | | | | | | | | |
|---|---|---|---|---|---|---|---|---|---|---|---|---|---|
| Ni-Cr, $MoSi_2$ | | Ni, $MoSi_2$ | | 30%Ni-70%$MoSi_2$ | | Mo Ni Si | | $Ni_{16}Cr_6Si_7$ | | Ni | | $MoSi_2$ | |
| Int. | d | Int. | d | Int. | d | Int. | d | Int. | d | Int. | d | Int. | d |
| | | | | | | | | 6 | 5.56 | | | | |
| | | | | W | 3.89 | | | | | | | 10 | 3.91 |
| | | | | | | | | 4 | 3.20 | | | | |
| | | | | S | 2.94 | | | | | | | 20 | 2.94 |
| | | | | | | | | 10 | 2.79 | | | | |
| W | 2.77 | VW | 2.78 | VW | 2.76 | 12 | 2.77 | | | | | | |
| | | | | | | | | 4 | 2.55 | | | | |
| | | | | VW | 2.50 | | | 6 | 2.49 | | | | |
| S | 2.36 | VS | 2.37 | VS | 2.36 | 60 | 2.38 | | | | | | |
| VW | 2.27 | | | | | | | 6 | 2.28 | | | | |
| | | | | S | 2.25 | | | | | | | 50 | 2.24 |
| S | 2.14 | VS | 2.15 | VS | 2.14 | 100 | 2.15 | 90 | 2.15 | | | | |
| | | | | W | 2.05 | 12 | 2.04 | | | | | | |

| Infiltration | | | | Mixed Powders | | | | | | | | | | | |
|---|---|---|---|---|---|---|---|---|---|---|---|---|---|---|---|
| Ni-Cr, $MoSi_2$ | | Ni, $MoSi_2$ | | 30%Ni-70%$MoSi_2$ | | Mo Ni Si | | $Ni_{16}Cr_6Si_7$ | | Ni | | $MoSi_2$ | |
| Int. | d | Int. | d | Int. | d | Int. | d | Int. | d | Int. | d | Int. | d |
| M | 2.05 | S | 2.05 | VS | 2.03 | | | | | 100 | 2.03 | | |
| VS | 2.00 | VS | 2.01 | VS | 2.01 | 100 | 2.01 | | | | | 60 | 2.01 |
| | | | | S | 1.98 | 60 | 1.98 | | | | | | |
| VS | 1.97 | VS | 1.97 | W | 1.97 | | | 100 | 1.97 | | | | |
| | | W | 1.93 | VW | 1.88 | | 1.89 | 30 | 1.89 | | | 20 | 1.94 |
| VW | 1.85 | | | | | | | 20 | 1.86 | | | | |
| VW | 1.79 | W | 1.78 | | | 6 | 1.81 | | | | | | |
| | | | | | | | | 6 | 1.77 | 42 | 1.76 | | |
| VW | 1.71 | | | M | 1.72 | 6 | 1.72 | 16 | 1.70 | | | | |
| | | | | | | | | 6 | 1.68 | | | | |
| | | | | M | 1.60 | | | 4 | 1.60 | | | 25 | 1.59 |
| | | | | M | 1.48 | | | | | | | 20 | 1.46 |
| VW | 1.43 | VW | 1.43 | VW | 1.44 | 6 | 1.44 | 6 | 1.45 | | | | |
| W | 1.42 | | | W | 1.42 | 25 | 1.42 | | | | | | |
| M | 1.37 | W | 1.37 | M | 1.37 | 25 | 1.38 | 10 | 1.40 | | | 25 | 1.39 |
| | | | | | | | | 4 | 1.34 | | | | |

| Infiltration | | | | Mixed Powders | | | | | | | | | | | |
|---|---|---|---|---|---|---|---|---|---|---|---|---|---|---|---|
| Ni-Cr, $MoSi_2$ | | Ni, $MoSi_2$ | | 30%Ni-70%$MoSi_2$ | | Mo Ni Si | | $Ni_{16}Cr_6Si_7$ | | Ni | | $MoSi_2$ | |
| Int. | d | Int. | d | Int. | d | Int. | d | Int. | d | Int. | d | Int. | d |
| S | 1.32 | S | 1.32 | S | 1.32 | 75 | 1.32 | 40 | 1.31 | | | 15 | 1.30 |
| M | 1.28 | M | 1.29 | M | 1.29 | 60 | 1.29 | 30 | 1.29 | | | | |
| | | | | | | | | 2 | 1.28 | | | | |
| | | | | S | 1.25 | 12 | 1.26 | 4 | 1.25 | 21 | 1.25 | 100 | 1.24 |
| M | 1.22 | M | 1.22 | M | 1.22 | 75 | 1.22 | 60 | 1.22 | | | 8 | 1.23 |
| | | | | | | 12 | 1.20 | | | | | | |
| S | 1.18 | S | 1.18 | M | 1.19 | 75 | 1.18 | 6 | 1.18 | | | | |
| | | | | | | | | 80 | 1.17 | | | | |
| | | | | M | 1.13 | 25 | 1.14 | | | | | 50 | 1.12 |
| W | 1.08 | W | 1.08 | W | 1.09 | 50 | 1.09 | | | | | 13 | 1.08 |
| W | 1.07 | | | W | 1.08 | 50 | 1.07 | | | | | | |
| | | | | W | 1.06 | | | | | 20 | 1.06 | 30 | 1.05 |
| S | 1.04 | VS | 1.04 | M | 1.04 | 100 | 1.04 | | | | | | |
| | | | | | | 12 | 1.03 | | | | | | |
| M | 1.02 | W | 1.02 | VW | 1.02 | 75 | 1.02 | | | 7 | 1.02 | | |
| W | 1.00 | VW | 1.01 | W | 1.01 | 75 | 1.00 | | | | | 80 | 1.00 |

| Infiltration | | | | Mixed Powders | | | | | | | | | | | |
|---|---|---|---|---|---|---|---|---|---|---|---|---|---|---|---|
| Ni-Cr, $MoSi_2$ | | Ni, $MoSi_2$ | | 30%Ni-79%$MoSi_2$ | | Mo Ni Si | | $Ni_{16}Cr_6Si_7$ | | Ni | | $MoSi_2$ | |
| Int. | d | Int. | d | Int. | d. | Int. | d | Int. | d | Int. | d | Int. | d |
| W | 0.98 | | | W | 0.99 | 60 | 0.99 | | | | | 25 | 0.98 |
| | | | | W | 0.98 | 25 | 0.98 | | | | | 25 | 0.98 |
| | | | | | | | | | | | | 25 | 0.97 |
| | | | | | | | | | | | | 25 | 0.90 |
| | | W | 0.88 | M | 0.88 | | | | | 4 | 0.88 | 35 | 0.88 |
| | | VW | 0.86 | | | | | | | 14 | 0.81 | | |
| | | | | | | | | | | 15 | 0.79 | | |

## Appendix 3

### Electric Characteristics of Coils Used in the Induction Furnace

Dimensions of Coils Used

| | Coil 1 | Coil 2 |
|---|---|---|
| Radius r, in. | 1.75 | 1.60 |
| Length l, in. | 88 | 145 |
| Number of turns n | 8 | 14 |

Calculation of Inductances

The approximate formula $L = \frac{(nr)^2}{9r + 10l}$ $\mu h$ was used for this calculation.

$$L_1 = \frac{(8 \times 1.75)^2}{(9 \times 1.75) + (10 \times 88)} = 0.219 \ \mu h$$

$$L_2 = \frac{(14 \times 1.60)^2}{(9 \times 1.60) + (10 \times 145)} = 0.351 \ \mu h$$

When coil 1 was replaced by coil 2, the inductance of system was increased by $L_2 - L_1 = 0.132 \ \mu h$. The expression for the frequency of oscillation of the system is

$$f = \frac{159}{\sqrt{LC}}$$

The frequency of oscillation decreased when L was increased. A decrease in f, in turn, caused a decrease in the excitation current, which hindered the oscillators from operating. By adjusting the excitation current, it was possible to bring the oscillators to normal operation.

## Appendix 4

### Thermodynamic Calculations on the Mo-Ni-Si System

The experimental data obtained in this investigation showed that the compound MoNiSi is stable at lower temperatures (below 1000° C). In view of these results, thermodynamic calculations were made on the Mo-Ni-Si system to obtain some indication of the criterion of stability in this system. As the compound initially present was $MoSi_2$ and the final one was MoNiSi, it was decided to develop a comparative thermodynamic study of the stability of the two compounds, and from this study to derive original thermodynamic data for the compound MoNiSi.

In the derivation it will be assumed that the coefficient of interaction $E_{Si}^{Mo}$ in the system Mo-Ni-Si is zero.

The basic equations to be considered are:

$$MoSi_{2(s)} \longrightarrow \underline{Mo}_{(l)} + 2\,Si_{(l)} \qquad (1)$$

$$\underline{Mo}_{(l)} + Ni_{(l)} + Si_{(l)} \longrightarrow MoNiSi_{(s)} \qquad (2)$$

where Mo, Si, and Ni represent the metals in the liquid solution.

To find the free energy change due to reaction 1 in its standard state, the following partial reactions are considered:

$$Mo_{(s)} + 2Si_{(s)} \longrightarrow MoSi_{2\,(s)} \quad (3)$$

$$Mo_{(l)} \longrightarrow Mo_{(s)} \quad (4)$$

$$2Si_{(l)} \longrightarrow 2Si_{(s)} \quad (5)$$

Adding both sides of equations 3, 4, and 5 results in

$$Mo_{(l)} + 2Si_{(l)} \longrightarrow MoSi_{2(s)} \quad (6)$$

The free energy changes of the reactions 3, 4, and 5, according to Hultgren and others (1971) are:

$$\Delta G^{o}_{R3} = -31,656 + 2.304\ T$$

$$\Delta G^{o}_{R4} = -\ 6,650 + 2.3\ T$$

$$\Delta G^{o}_{R5} = -24,164 + 14.34\ T$$

The overall free energy change, corresponding to reaction 6 will therefore be

$$\Delta G^{o}_{R6} = \Delta G^{o}_{R3} + \Delta G^{o}_{R4} + \Delta G^{o}_{R5} = -62,470 + 18.944\ T$$

However, reaction 1 is the reverse of reaction 6.

Therefore:

$$\triangle G^{o}_{R1} = -\triangle G^{o}_{R6} = 62{,}470 - 18.944\ T \qquad (7)$$

For reaction 1:

$$\triangle G^{o}_{R1} = -Rt \ln \frac{a_{Mo} \cdot a^2_{Si}}{a_{MoSi_2}} = -Rt \ln (a_{Mo} \cdot a^2_{Si}) \qquad (8)$$

Let $\triangle G^{o}_{R1} = 62{,}470 - 18{,}944\ T = A + BT$

where

$$A = 62{,}470$$

$$B = -18.944$$

Equation 8 becomes:

$$\ln (a_{Mo} \cdot a^2_{Si}) = -\left(\frac{B}{R} + \frac{A}{RT}\right)$$

$$\ln a_{Mo} + \ln a_{Si} + \ln a_{Si} = -\left(\frac{B}{R} + \frac{A}{RT}\right)$$

or

$$\ln (a_{Mo} \cdot a_{Si}) = -\left(\frac{B}{R} + \frac{A}{RT}\right) - \ln a_{Si} \qquad (9)$$

Another simplifying assumption will have to be made here. It will be assumed that $a_{Si}$ in the Ni-Si system is analogous to $a_{Si}$ in the Fe-Si system. The difficulty here is that, apparently, data for the activities in the Ni-Si system are not available, according to

Hultgren and others (1971). The use of thermodynamic data from the Fe-Si system to replace those from the Ni-Si system is justified by the proximity of Fe and Ni in the periodic table. It seems reasonable to predict that the deviation from ideality is largely negative in Ni-Si, because it is large in Fe-Si; therefore, we think that the assumption made leads to a smaller error than if an ideal solution assumption were considered.

Making this assumption, it is possible to calculate $a_{Si}$, using the partial molar free energy of Si in Fe-Si:

$$\Delta\bar{G}_{Si} = RT \ln a_{Si}$$

where

$$\Delta\bar{G}_{Si} = \Delta\bar{H}_{Si} - \Delta\bar{S}_{Si}\, T$$

Assuming that $\Delta\bar{H}_{Si}$ and $\Delta\bar{S}_{Si}$ do not vary with temperature, we obtain, from Hultgren and others (1971):

$$\Delta\bar{G}_{Si} = -\ 23{,}488 + 1.566\ T, \text{ for } N_{Si} = 0.24$$

Therefore

$$\ln a_{Si} = \frac{-23{,}488}{RT} + \frac{1.566}{R}$$

Therefore, equation 9 becomes:

$$\ln(a_{Mo} \cdot a_{Si}) = -\frac{B}{R} - \frac{A}{RT} - \left( \frac{-23,488}{RT} + \frac{1.566}{R} \right)$$

$$\ln(a_{Mo} \cdot a_{Si}) = -\left( \frac{B}{R} + \frac{1.566}{R} \right) - \left( \frac{A}{RT} - \frac{23,488}{RT} \right) \qquad (10)$$

For reaction 2:

$$\Delta G^{o}_{fMoNiSi} = -RT \ln \frac{a_{MoNiSi}}{a_{Mo} \cdot a_{Ni} \cdot a_{Si}}$$

$$= RT \ln (a_{Mo} \cdot a_{Ni} \cdot a_{Si})$$

$$\text{Let } \Delta G^{o}_{fMoNiSi} = C + DT \qquad (11)$$

Therefore

$$C + DT = RT \ln (a_{Mo} \cdot a_{Ni} \cdot a_{Si})$$

$$\ln (a_{Mo} \cdot a_{Ni} \cdot a_{Si}) = \left( \frac{D}{R} + \frac{C}{RT} \right) \qquad (12)$$

Here a simplifying assumption will be made. We will assume that the solution $Mo_{(l)} + Si_{(l)}$ behaves as an ideal solution, setting

$$a_{Ni} \cong N_{Ni}$$

where $N_{Ni}$ is the atom fraction of nickel in the solution. In the experiment, the atom fractions of the metals present were

a/o Ni = 0.63

a/o Si = 0.24

a/o Mo = 0.13

The assumption made seems reasonable since the system is rich in nickel. The assumption made is that Raoult's law is applicable.

Equation 12 becomes:

$$\ln (a_{Mo} \cdot a_{Si}) = \left(\frac{D}{R} + \frac{C}{RT}\right) - \ln N_{Ni} = \left(\frac{D}{R} - \ln N_{Ni}\right) + \frac{C}{RT} \quad (13)$$

Comparing equations 10 and 13, one obtains:

$$\frac{D}{R} - \ln N_{Ni} = -\left(\frac{B}{R} + 1.566\right)$$

and

$$\frac{C}{R} = -\left(\frac{A}{R} - \frac{23,488}{R}\right)$$

or

$$\frac{D}{R} + 0.46 = -\left(\frac{-18,944}{1.987} + \frac{23,488}{1.987}\right) = 8.75$$

$$D = 16.46$$

$$\frac{C}{R} = \left(\frac{62,470}{R} - \frac{23,488}{R}\right)$$

$$C = -38,980$$

Therefore, the free energy of formation of MoNiSi will be given by

$$\triangle G^{o}_{fMoNiSi} = -38,980 + 16.46\ T$$

Taking Si as the reference for comparing the free energies of formation of MoNiSi and $MoSi_2$, it follows that

$$\triangle G^{o}_{f\frac{1}{2}MoSi_2} = -31,235 + 9.472\ T \qquad (14)$$

$$\triangle G^{o}_{fMoNiSi} = -38,980 + 16.46\ T \qquad (15)$$

The equilibrium temperature indicated by equations 14 and 15 for the compounds $MoSi_2$ and MoNiSi is approximately 1100°K, significantly below the temperatures at which the formation of MoNiSi actually occurred in the experimentation. An examination of the two straight lines plotted in figure 16, however, shows that relatively small errors in the estimated coefficients would cause considerable shift in the theoretical equilibrium temperature. This is, of course, due to the fact that the slopes of the two lines are similar.

It is, therefore, considered that equation 15 can be taken as an estimate for the free energy of formation of the compound MoNiSi.

## LITERATURE CITED

Allen, B. C., and Kingery, W. D., 1959, Surface tension and contact angles in some liquid metal-solid ceramic systems at elevated temperatures: Transactions Metallurgical Society of AIME, v. 215, no. 2, p. 30-37.

Amberg, S., 1961, Studies on the sintering of $MoSi_2$ - $Al_2O_3$ cermets: Powder Metallurgy, no. 8, p. 101-112.

Blakeley, T. H.,and White, A. E. S., 1956: second Plansee seminar, 1955, Proceedings.

Clauss, F. J., 1969, Engineer's guide to high-temperature materials: Reading, Addison-Wesley Publishing Company, 401 p.

Davies, J. T., and Rideal, E. K., 1963, Interfacial phenomena: New York, Academic Press, 480 p.

Dotson, C. L., and Kotfila, R. J., 1969, The behavior of composite Ag-infiltrated tungsten up to 5000°F: Metallurgical Society of AIME, Refractory Metals and Alloys, IV-Research and Development, French Lick, 1965, p. 1209-1227.

Gatti, A., Berry, J. M., Gebhardt, J. J., Mullin, J., and Feingold, E., 1967, Investigation of the reinforcement of ductile metals with strong, high modules, discontinuous brittle fibers, in Sutton, W. H., 1969, Review of research on composite materials: Los Angeles, Report for the 15th Refractory Composites Working Group, p. 1-24.

Gladyshevskii, E. I., and Kuz'ma, Y. B., 1960, Crystal structure of ternary phases in the Mo (W) - Fe (Co, Ni) - Si systems: Zhur. Strukt. Khim., v. 1, no. 1, p. 66-71.

Gladyshevskii, E. I., and Borusevich, Y., 1963, Russian Journal of Inorganic Chemistry, v. 8, p. 997-1000.

Glaser, F. W., 1955, Progress report on cermets: Metal Progress, v. 67, no. 4, p. 77-82.

Goetzel, C. G., and Adamec, J. B., 1956, Infiltration of cermets for improved toughness: Metal Progress, v. 68, no. 12, p. 101-106.

Goetzel, C. G., and Skolnick. L. P., 1956: Second Plansee Seminar, 1955, Proceedings.

Goetzel, C. G., 1960, Infiltration process in Tinklepaugh, J. R., and Crandall, W. B., 1960, Cermets: New York, Reinhold Publishing Corporation, p. 73-81.

Goetzel, C. G., and Rittenhouse, J. B., 1964, The influence of processing conditions on the properties of Ag-infiltrated W: International Symposium on Powder Metallurgy, Paris, June 1964.

Goetzel, C. G., and Shaler, A. J., 1964, Mechanism of infiltration of porous powder-metallurgy parts: Journal of metals, November 1964, p. 901-905.

Graham, J., Weymouth, J. H., and Williams, L. S., 1963, Fundamental and technological aspects of infiltrated oxide cermets: The Journal of the Australian Institute of Metals, v. 8, no. 3, p. 280-297.

Guard, R. W., and Smith, E. A., 1959, Constitution of nickel-base ternary alloys: Journal of the Institute of Metals, v. 88, p. 283-287.

Harding, F. L., 1968, Wetting of ceramic oxides by indium, gallium, tin and silver: London, College of Ceramics at Alfred University.

Hultgren, R., Orr, R. L., and Kelley, K. K., 1971, Supplement to selected values of thermodynamic properties of metals and alloys (current loose-leaf sheets): Berkeley, California, Inorganic Materials Research Division, Lawrence Radiation Laboratory, University of California.

Kieffer, R., and Kölbl, F., 1950, Berg-u hüttenmänn Monatsh, v. 95, no. 49.

Kimura, T., Kosco, J. C., and Shaler, A. J., 1959, Detergency during infiltration in powder metallurgy: 15th Annual Meeting Metal Powder Industries, New York 1959, Report.

Krol, J. M., and Goetzel, C. G., 1949, Air Force Technical Report 5892.

Manning, C. R., and Stoops, R. F., 1968, High-temperature cermets: II, Wetting and fabrication: Journal of the American Ceramic Society, v. 51, no. 8, p. 415-519.

Matt, R. E., and Warga, J. J., 1964, Development of silver-inviltrated nozzle for uncooled rocket motors: Fifth Plansee Seminar, 1964, Proceedings.

Naidich, Y. V., and Nevodnik, G. M., 1969, Wettability of the surface of SiC single crystals by metallic melts: Izvest. Akad. Nauk SSSR, Neorg. Materialy, no. 12, p. 2066-2070.

Pfautsch, 1925, Über das Dreistoffsystem Mo-Ni-Si: Zeitschrift für Metallkunde, v. 17, p. 48-52.

Pozzo, R. F., and West, I. V., 1960, Chromium carbide applications, in Tinklepaugh, J. R., and Crandal, W. B., Cermets: New York, Reinhold Publishing Corporation, p. 151-158.

Samsonov, G. V., 1964, High-temperature materials, no. 2, properties index: New York, Plenum Press.

Samsonov, G. V., Panasyuk, A. D., and Kozina, G. K., 1968, Wetting of refractory carbides with liquid metals: Poroshkovaya Metallurgiya, no. 71, p. 42-48.

Shaler, A. J., 1965, Theoretical aspects of the infiltration of powder metallurgy products: Int. Jour. of Powder Metallurgy, v. 1, no. 1, p. 3-13.

Wehrmann, R., 1967, Silicides, in Campbell, J. E., and Sherwood, E. M., High-temperature materials and technology: New York, John Wiley & Sons, Inc., p. 399-430.

Williams, L. S., 1965, Infiltrated oxide cermets, in Popper, P., Special ceramics 1964: New York, Academic Press, p. 147-165.